Am J Physiol Lung Cell Mol Physiol 312: L609–L624, 2017.
First published February 17, 2017; doi:10.1152/ajplung.00531.2016.

RESEARCH ARTICLE

Central role of T helper 17 cells in chronic hypoxia-induced pulmonary hypertension

Levi D. Maston,[1] David T. Jones,[1] Wieslawa Giermakowska,[1] Tamara A. Howard,[1] Judy L. Cannon,[2] Wei Wang,[3] Yongyi Wei,[3] Weimin Xuan,[3] Thomas C. Resta,[1] and Laura V. Gonzalez Bosc[1]

[1]*Vascular Physiology Group, Department of Cell Biology and Physiology, University of New Mexico, Albuquerque, New Mexico;* [2]*Department of Molecular Genetics and Microbiology, University of New Mexico, Albuquerque, New Mexico; and* [3]*Department of Chemistry, University of New Mexico, Albuquerque, New Mexico*

Submitted 1 December 2016; accepted in final form 9 February 2017

Maston LD, Jones DT, Giermakowska W, Howard TA, Cannon JL, Wang W, Wei Y, Xuan W, Resta TC, Gonzalez Bosc LV. Central role of T helper 17 cells in chronic hypoxia-induced pulmonary hypertension. *Am J Physiol Lung Cell Mol Physiol* 312: L609–L624, 2017. First published February 17, 2017; doi:10.1152/ajplung.00531.2016.—Inflammation is a prominent pathological feature in pulmonary arterial hypertension, as demonstrated by pulmonary vascular infiltration of inflammatory cells, including T and B lymphocytes. However, the contribution of the adaptive immune system is not well characterized in pulmonary hypertension caused by chronic hypoxia. $CD4^+$ T cells are required for initiating and maintaining inflammation, suggesting that these cells could play an important role in the pathogenesis of hypoxic pulmonary hypertension. Our objective was to test the hypothesis that $CD4^+$ T cells, specifically the T helper 17 subset, contribute to chronic hypoxia-induced pulmonary hypertension. We compared indices of pulmonary hypertension resulting from chronic hypoxia (3 wk) in wild-type mice and recombination–activating gene 1 knockout mice ($RAG1^{-/-}$, lacking mature T and B cells). Separate sets of mice were adoptively transferred with $CD4^+$, $CD8^+$, or T helper 17 cells before normoxic or chronic hypoxic exposure to evaluate the involvement of specific T cell subsets. $RAG1^{-/-}$ mice had diminished right ventricular systolic pressure and arterial remodeling compared with wild-type mice exposed to chronic hypoxia. Adoptive transfer of $CD4^+$ but not $CD8^+$ T cells restored the hypertensive phenotype in $RAG1^{-/-}$ mice. Interestingly, $RAG1^{-/-}$ mice receiving T helper 17 cells displayed evidence of pulmonary hypertension independent of chronic hypoxia. Supporting our hypothesis, depletion of $CD4^+$ cells or treatment with SR1001, an inhibitor of T helper 17 cell development, prevented increased pressure and remodeling responses to chronic hypoxia. We conclude that T helper 17 cells play a key role in the development of chronic hypoxia-induced pulmonary hypertension.

CD4 T cells; inflammation; interleukin-6; SR1001; retinoid-related orphan receptor-γτ

CHRONIC HYPOXIA (CH)-induced pulmonary hypertension (PH) is associated with respiratory diseases such as chronic obstructive pulmonary disease (COPD) (36, 47). PH greatly affects the outcome of COPD (8). Medical regimens for hypoxic PH are currently limited to supportive therapy (42).

Hypoxia induces a pulmonary artery-specific inflammatory environment, with an accumulation of lymphocytes in the lungs that may contribute to vascular remodeling in rats (9, 40, 50). COPD is also characterized by an abnormal inflammatory response (44, 60) with increased circulating $CD4^+$ T cells (60). Therefore, $CD4^+$ T cells have the potential to play a significant role in the disease process initiated by hypoxia.

$CD4^+$ T cells are responsible for orchestrating immune processes and are critical in amplifying inflammatory responses by other effector immune cells (21). $CD4^+$ T cells can differentiate into distinct effector subsets, including T helper 1 (T_H1), T helper 2 (T_H2), and T helper 17 (T_H17) cells and T regulatory cells (Tregs). T_H17 cells are increased in the lungs of patients with COPD (56). It is unknown whether this response is a consequence of cigarette smoking or hypoxemia. Exposure of naïve T cells to hypoxic conditions favors differentiation into T_H17 cells (14). Furthermore, T_H17 cell number increases in lungs of mice exposed to 3 days of CH (23). Although the presence of T_H17 cells has been associated with PH (23, 25), whether T_H17 cells can directly induce PH is still unknown. Furthermore, studies suggest that Tregs function to limit vascular injury and may protect against the development of pulmonary arterial hypertension (PAH) and CH-induced PH (12, 53).

Based on these findings, we hypothesized that $CD4^+$ T cells, specifically T_H17 cells, contribute to the development of CH-induced PH. This study identified a critical role for T_H17 cells as mediators of pulmonary arterial inflammation and PH following CH exposure.

METHODS

Animals. C57BL/6 $RAG1^{-/-}$ (male and female, 25–28 g), C57BL/6 wild-type (WT; sex and age matched), and C57BL/6-Il17a^{tm1Bsgen}/J mice (The Jackson Laboratory) were used in these studies. Protocols were approved by the Institutional Animal Care and Use Committee of the University of New Mexico Health Sciences Center.

Chronic hypoxia exposure. Mice exposed to CH were housed in a hypobaric chamber (~380 mmHg, 2–21 days). Control mice were housed at ambient barometric pressure (normoxia, N; ~630 mmHg).

Assessment of right ventricular systolic pressure and right ventricular hypertrophy. Peak right ventricular systolic pressure (RVSP) was assessed in isoflurane-anesthetized mice, as described previously (41). RV systolic pressure (RVSP) was measured as an index of pulmonary arterial pressure in anesthetized mice (2% isoflurane and 98% O_2 gas mixture). An upper transverse laparotomy was performed to expose the diaphragm. A 25-gauge needle connected to a pressure transducer (model P23 XL; Spectramed) was inserted into the RV via a closed-

Address for reprint requests and other correspondence: L. V. Gonzalez Bosc, MSC08 4750 1, Biomedical Research Facility 237J, University of New Mexico, Albuquerque, NM 87131 (e-mail: lgonzalezbosc@salud.unm.edu).

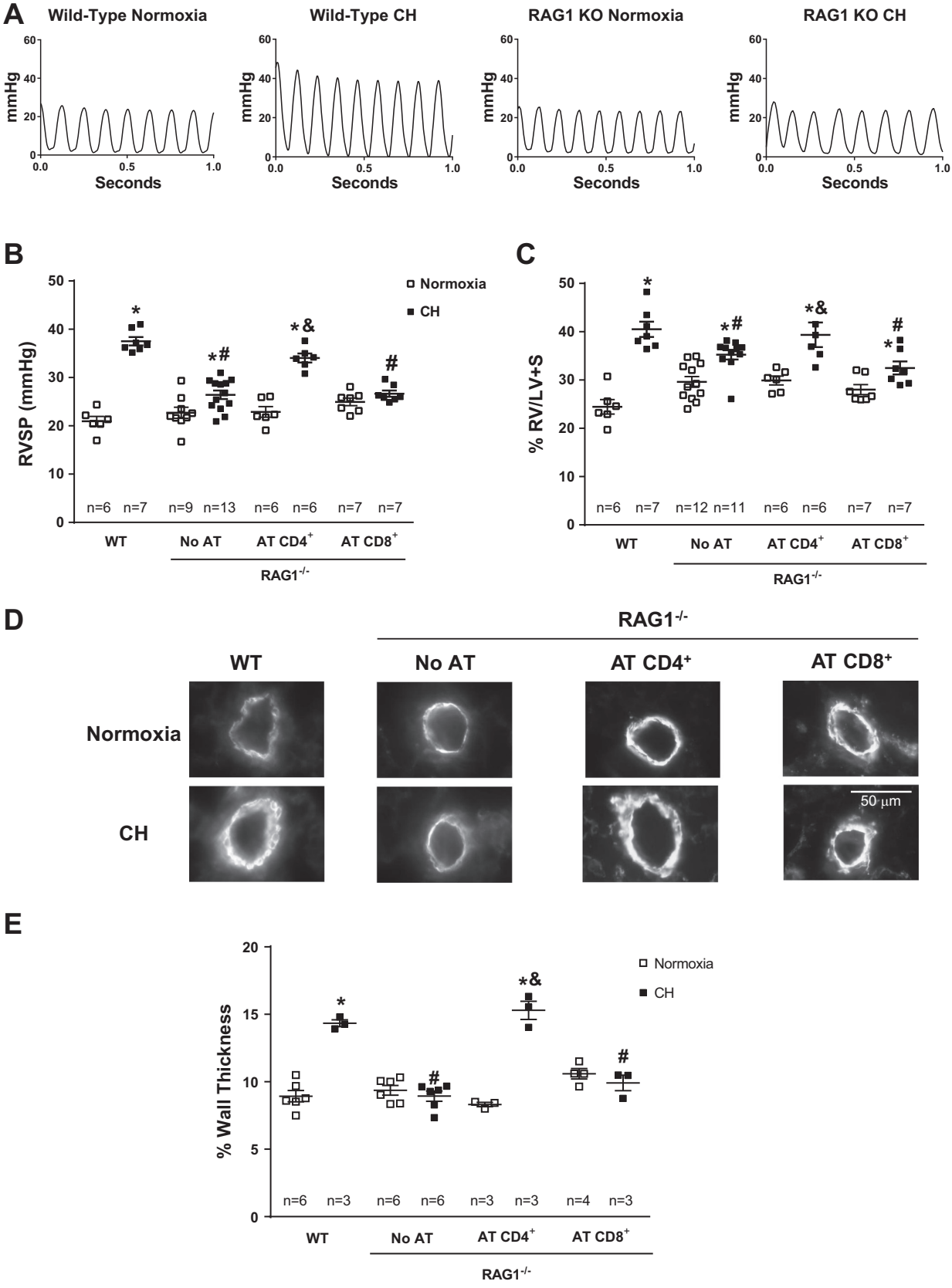

Table 1. *Biometrics of WT and RAG1$^{-/-}$ mice exposed to normoxia or CH, with or without the adoptive transfer of CD4$^+$ or CD8$^+$ T cells*

Treatment	Exposure	HR, beats/min	Hto, %	BW, g	LV + S/BW, mg/g	RV/BW, mg/g	*n* (mice)	*n* (females)
WT	Normoxia	388 ± 13	41 ± 2	22.7 ± 1.0	3.04 ± 0.10	0.83 ± 0.08	7	3
WT	CH	407 ± 40	60 ± 2*	21.8 ± 0.9	3.65 ± 0.10*	1.50 ± 0.06*	7	3
No AT	Normoxia	377 ± 23	42 ± 2	28.1 ± 1.3	3.39 ± 0.08	0.92 ± 0.04	6	3
No AT	CH	413 ± 10	51 ± 3*	24.6 ± 1.3	3.46 ± 0.10	1.20 ± 0.10*#	6	3
CD4 AT	Normoxia	424 ± 20	40 ± 1	24.9 ± 1.3	2.88 ± 0.10	0.86 ± 0.04	6	3
CD4 AT	CH	383 ± 20	58 ± 1*	22.9 ± 1.6	3.44 ± 0.24	1.33 ± 0.04*	6	3
CD8 AT	Normoxia	408 ± 30	40 ± 1	26.7 ± 1.8	3.27 ± 0.11	0.92 ± 0.06	7	3
CD8 AT	CH	428 ± 16	53 ± 2*	23.3 ± 2.1	3.43 ± 0.20	1.10 ± 0.05#	7	3

Values are means ± SE. WT, wild-type; CH, chronic hypoxia; AT, adoptive transfer; HR, heart rate; Hto, hematocrit; BW, body weight; LV + S, left ventricle + septum; RV, right ventricle. *$P < 0.05$ vs. normoxia; #$P < 0.05$ vs. WT.

chest transdiaphragmatic approach and the output amplified by a Gould Universal amplifier. All data were recorded, and heart rate was calculated with a computer-based data acquisition system (ATCODAS; DATAQ Instruments). After hemodynamic data were collected, the heart was isolated and the atria and major vessels were removed. The RV was dissected from the left ventricle (LV) and septum (S). Right ventricular (RV) hypertrophy (Fulton's index) was expressed as the percentage ratio of RV to left ventricle plus septum (LV + S) weight and RV to body weight (BW).

Vascular morphometry. Pulmonary arterial remodeling (<150 μm outer diameter) was assessed using a modification of previously published methods (15). After collection of hemodynamic data, the lungs were perfused via the right ventricle with ~5 ml of modified physiological saline solution (HEPES-PSS, 134 mM NaCl, 6 mM KCl, 1 mM MgCl, 10 mM HEPES, 2 mM $CaCl_2$, 0.026 mM EDTA, and 10 mM glucose) containing heparin, 4% albumin (Sigma), and 10^{-4} M papaverine (Sigma) at 20 mmHg to maximally dilate and flush the circulation of blood. The heart, lungs, and trachea were removed in block. The right lobes were tied off, removed, and preserved in RNA Later. The left lobe of the blood-cleared lung was fixed in 4% paraformaldehyde (Polyscience, Warrington, PA) in phosphate-buffered saline (PBS) fixative.

Lung sections (5 μm) were stained with rabbit anti-smooth muscle α-actin (Ab5694; Abcam, Cambridge, MA) (39, 52) antibody or rabbit IgG control (negative) followed by DyLight 549-donkey anti-rabbit (Thermo Fisher Scientific). Sections were examined using a ×20 or ×40 objective on a Zeiss Axiovert 200M scope and images acquired with a Cool Snap EZ camera using NIS-Elements F 3.0 software. Images were analyzed with ImageJ (National Institutes of Health, Bethesda, MD). Vessels sectioned at oblique angles were excluded from analysis. The analysis was performed in arteries with <150 μm outer diameter. Approximately 10 arteries per animal were analyzed: %wall thickness = [(external diameter − luminal diameter)/external diameter] × 100. Diameters were calculated from the measured circumferences.

Immunohistochemistry and immunofluorescence. Sections from paraffin-embedded lungs were deparaffinized, rehydrated, washed, and subjected to antigen retrieval for 20 min at ≥90°C in a buffer containing 10 mM Tris, pH 9.0, + 1 mM EDTA in a rice cooker and blocked/permeabilized with 1× PBS + 2% normal goat serum + 0.1% Triton X-100. Lung sections were incubited with IgG control or rabbit anti-human CD3ε primary antibody (1:400; Dako A052, lot 20024875, stock 0.6 mg/ml) or anti-IL-6 (Ab6672; Abcam) (38) followed by rat anti-rabbit horseradish peroxidase-conjugated secondary antibody and signal development with diaminobenzidine.

Pulmonary arteries were identified based on morphology. The number of CD3$^+$ cells in the medial and perivascular regions was normalized to outer diameter. Only arteries with <150 μm outer diameter were analyzed. Samples from each time point were processed and analyzed right after each set of experiments; therefore, the results from different time points cannot be compared statistically. Mean gray values of IL-6 staining were quantified in the medial layer of pulmonary arteries using ImageJ.

For the detection of T_H17 cells, lung sections were incubated with control IgG or rabbit anti-IL-17 (1:400; AbCam ab79056, lot GR281497-1, stock 1 mg/ml) (26, 54, 59) overnight at 4°C, followed by secondary antibody donkey Alexa Fluor 488 anti-rabbit (1:300; Jackson 711-546-152, lot 124082) for 1 h at room temperature and fixed for 15 min with 1× PBS + 1% formaldehyde (EM grade). Then, the lung sections were incubated with rabbit anti-CD3ε (1:400; Dako A052, lot 20024875, stock 0.6 mg/ml) overnight at 4°C, followed by secondary antibody donkey DyLight 549 anti-rabbit (1:800; Jackson 711-505-052, lot 93339) for 1 h at room temperature. Sections were counterstained with 0.05 μM AlexaFluor 633 hydrazide to label the elastic lamina. Images were obtained using a Zeiss AxioPlan 2-Nuance Multi-Spectral Camera and unmixed to remove tissue auto fluorescence. A nonsharp mask filter was applied to the composite image using ImageJ.

For the detection of proliferating cells, lung sections were incubated with control IgG or with rabbit monoclonal anti-Ki-67 SP6 clone (1:500; ThermoFisher Scientific RM-9106-S0), and detection of apoptotic cells was done using a rabbit polyclonal anti-cleaved caspase 3 (1:250; Cell Signaling Technology 9661) antibody overnight at 4°C, followed by secondary antibody donkey DyLight 549 anti-rabbit. Sections were counterstained with SYTOX green to label nuclei and Alexa Fluor 633 hydrazide to label the elastic lamina. Images were acquired using a Leica TCS SP5 Spectral Confocal System.

Flow cytometry. A single-cell suspension from blood-cleared lungs was prepared by mincing and subsequent digestion with type IV

Fig. 1. CD4$^+$ T cells contribute to chronic hypoxia (CH)-induced pulmonary hypertension (PH). *A*: representative right ventricular (RV) systolic pressure (RVSP) traces from isoflurane-anesthetized wild-type (WT) and RAG1$^{-/-}$ mice without adoptive transfer (AT) or AT of enriched CD4$^+$ or CD8$^+$ T cells exposed to 21 days of CH or normoxia, as indicated. *B*: summary of peak RVSP data. *C*: %RV to left ventricle plus septum (%RV/LV + S) weight. Values are means ± SE; *n* = no. of animals. *$P < 0.05$ vs. normoxia; #$P < 0.05$ vs. CH WT; &$P < 0.05$ vs. CH RAG1$^{-/-}$. No AT, analyzed by 2-way ANOVA, followed by multiple-comparison Student-Newman-Keuls test. *D*: representative images of α-smooth muscle actin-labeled pulmonary artery sections with external diameters <150 μm from normoxic and CH (21 days) WT and RAG1$^{-/-}$ mice receiving either no adoptive transfer or adoptive transfer with enriched CD4$^+$ or CD8$^+$ T cells; scale bar, 100 μm. *E*: %wall thickness of pulmonary arteries from the groups described in *A*. Values are means ± SE; *n* = no. of animals; at least 10 arteries/animal were measured; *$P < 0.05$ vs. normoxia; #$P < 0.05$ vs. WT CH; &$P < 0.05$ vs. No AT CH, analyzed by 2-way ANOVA, followed by multiple comparisons Student-Newman-Keuls test.

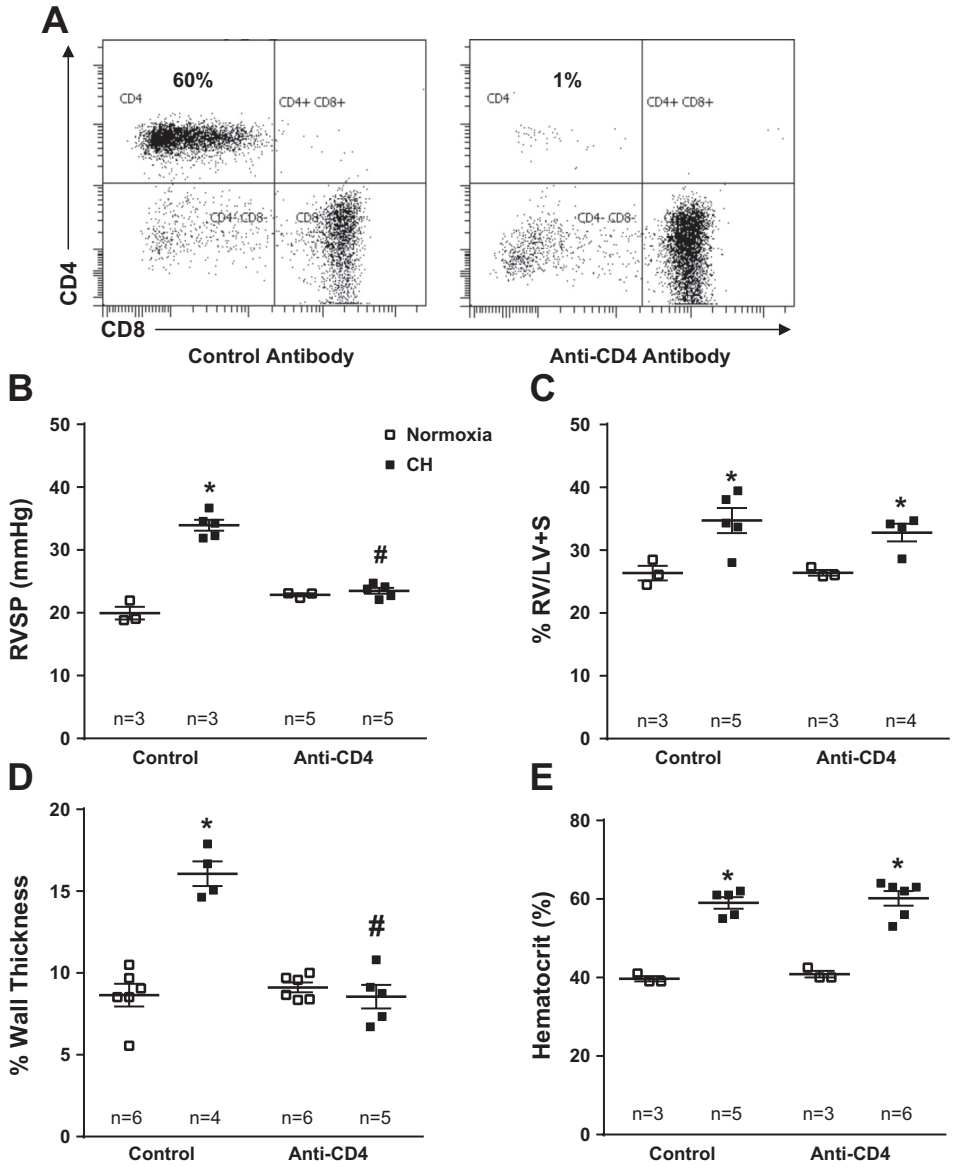

Fig. 2. $CD4^+$ cell depletion attenuates the development of CH-induced PH. Anti-CD4 or control antibody (2 mg/kg) given once/wk, starting 1 wk before CH (21 days). *A*: representative flow cytometry plots of splenocytes labeled for CD3 (gated), CD4, and CD8. *B*: peak RVSP. *C*: Fulton's index. *D*: %wall thickness. *E*: hematocrit. Values are means ± SE. $*P < 0.05$ vs. normoxia; $\#P < 0.05$ vs. CH control (n = no. of animals, and in *D* at least 10 arteries/animal were measured; 2-way ANOVA followed by multiple-comparison Student-Newman-Keuls test).

collagenase, elastase, and hyaluronidase (Sigma) in RPMI 1640 for 1 h at 37°C (34). The digested lungs were pushed through a Falcon 70-μm cell strainer and washed in MACS buffer (PBS, 0.5% BSA, 2 mM EDTA). Any remaining red blood cells were lysed with a hypotonic lysing buffer (8,024 mg/l NH_4Cl, 1,001 mg/l $KHCO_3$, and 3.722 mg/l EDTA) for 30 s on ice. Cells were incubated for 4 h with phorbol 12-myristate 13-aceate (50 ng/ml), ionomycin (1 μg/ml), and a protein transport inhibitor (GolgiStop with monensin; BD Biosciences) before immunostaining to enhance the sensitivity of IL-17A detection. FC receptors were blocked with anti-CD32/CD16 antibody (rat IgG_{2b} anti-mouse CD16/CD32 monoclonal, 101330; BD Biosciences, San Jose, CA) for 10 min at room temperature. Cells were washed and stained with PerCP/Cy5.5 anti-mouse CD4 (clone GK1.5, 100432; BioLegend, San Diego, CA), APC/Cy7 anti-mouse CD3ε (clone 145-2C11, 100330; BioLegend), and PE anti-mouse IL-17A (clone TC11-18H10.1, 506910; BioLegend) or PE anti-mouse/rat/human FoxP3 (clone 150D, 32008, BioLegend) for 1 h at 4°C in the dark. Macrophages were detected by staining the lung digest with APC anti-mouse CD45 (103112; BioLegend), PE/Cy7 anti-mouse F4/80 (123114, BioLegend, San Diego, CA), and Alexa

Table 2. *Biometrics of WT mice treated with either control antibody or anti-CD4 antibody*

Treatment	Exposure	HR, beats/min	Hto, %	BW, g	LV + S/BW, mg/g	RV/BW, mg/g	*n* (mice)
Control	Normoxia	407 ± 24	39.7 ± 0.7	28.1 ± 1.0	2.97 ± 0.28	0.78 ± 0.01	3
Control	CH	365 ± 47	59.0 ± 1.4*	27.0 ± 0.6	3.72 ± 0.19	1.23 ± 0.05*	6
Anti-CD4	Normoxia	421 ± 27	40.8 ± 0.4	31.1 ± 2.4	2.90 ± 0.26	0.77 ± 0.06	3
Anti-CD4	CH	399 ± 10	60.2 ± 1.9*	26.3 ± 0.7*	3.73 ± 0.27	1.23 ± 0.04*	6

Values are means ± SE. Only male mice were used. WT, wild-type; AT, adoptive transfer; HR, heart rate; Hto, hematocrit; BW, body weight; LV + S, left ventricle + septum; RV, right ventricle; CH, chronic hypoxia. $*P < 0.05$ vs. normoxia.

Fluor 488 anti-mouse CD11c (117311; BioLegend) for 1 h at 4°C in the dark.

T cell polarization. Lymphocyte populations were isolated from lymph nodes by negative selection according to Miltenyi Biotec Magnetic Cell Sorting T Cell Isolation kits. Cell enrichment was assessed by flow cytometry. Since T_H17 cells lack unique surface markers, $CD4^+$ T cells were purified as described above from C57BL/6-Il17a^{tm1Bsgen}/J mice, which express enhanced green fluorescence protein (EGFP) in cells expressing IL-17A. $CD4^+$ T cells were polarized to T_H17 cells, following a published protocol (57) by placing them in six-well culture dishes precoated with anti-mouse CD3ε clone 145-2c11 (2 μg/ml). The cells were cultured for 3 days in the presence of anti-mouse CD28 (5 μg/ml), IL-6 (50 ng/ml), TGF-β1 (1 ng/ml), anti-mouse IL-4 (10 μg/ml), anti-mouse IFN-γ (10 μg/ml), and mouse IL-23 (5 ng/ml; BioLegend). On *day 3*, cells were separated using automatic fluorescence-activated cell sorting based on EGFP fluorescence intensity.

T cell subset adoptive transfer. Approximately 250,000 complete (naïve and memory) $CD4^+$ or $CD8^+$ T cells were transferred to RAG1-knockout (KO) mice via retro-orbital injection (13). Approximately 10,000 T_H17 cells were adoptively transferred to RAG1-KO mice using the retro-orbital approach. All RAG1$^{-/-}$ mice received the adoptive transfer of T cell subsets or saline 2 wk before they were exposed to normoxia or CH for 3 wk. Mice were monitored for 2 wk following adoptive transfer and weighed periodically to ensure health before exposure to CH or normoxia. Following hemodynamic measurements at the conclusion of the experiments, spleens were removed and splenocytes processed for flow cytometry to verify successful engraftment of adoptively transferred lymphocytes.

$CD4^+$ T cell depletion. Rat anti-mouse CD4 (clone GK1.5) antibody or control purified IgG2b isotype control (Biolegend) was injected into mice (4 μg/g body wt ip) 7 days before CH exposure and weekly for an additional 3 wk (22). Following the experiments, $CD4^+$ T cell depletion was assessed using flow cytometry on single-cell suspensions of splenocytes.

Drug treatment. SR1001 [*N*-(5-(*N*-(4-(1,1,1,3,3,3-hexafluoro-2-hydroxypropan-2-yl) phenyl) sulfamoyl)-4-methylthiazol-2-yl) acetamide], a synthetic inverse agonist specific for retinoid-related orphan receptor (ROR)α and RORγτ (K_is = 172 and 111 nM, respectively), was synthesized in house (49). SR1001 (5, 49) was dissolved in propylene glycol (vehicle) and injected subcutaneously (sc) for 5 days during normoxia or CH exposure (25 mg·kg^{-1}·day^{-1}). For the prevention study, vehicle or SR1001 was delivered by osmotic pump for 21 days during normoxia or CH exposure. For the reversal study, mice were exposed to CH for 21 days, and then osmotic pumps containing vehicle or SR1001 were implanted and mice treated for 14 days during CH exposure. Both RORα and RORγ have roles outside of the immune system and are critical regulators of hepatic metabolism. It has been reported that SR1001 administration to C57BL/6 mice suppressed the expression of hepatic ROR target genes *Cyp7b1*, *Nr1d1* (also called *Rev-erbα*), and *Serpine1* (also called *PAI-1*), indicating that this class of compound may have metabolic effects; however, no obvious toxicity was observed in animals treated with SR1001 (49). We also did not observe any obvious toxicity in mice treated with SR1001.

Pulmonary artery smooth muscle cell migration and confluency assay. Primary pulmonary arterial smooth muscle cell (PASMC) cultures were established and cells authenticated as described previously (27, 37). PASMC were plated on gelatin-coated dishes and cultured in smooth muscle cell medium (Cell Biologics) containing 10% fetal bovine serum and antibiotic-antimycotic solution in a humidified atmosphere of 5% CO_2-95% air at 37°C. To measure cell migration or cell numbers, an IncuCyte (Essen Bioscience) live-cell imaging system was used. Before experiments, PASMCs were cultured for ≥48 h in serum-free smooth muscle cell medium containing insulin, EGF, hydrocortisone, L-glutamine, and antibiotic-antimycotic solution (M2268SF; Cell Biologics). Migration was determined by using a WoundMaker (Essen Bioscience) to produce homogenous, 700- to 800-μm-wide scratch wounds on a confluent monolayer of PASMC. Cell count was assessed by determining the confluency of the culture over time divided by the initial confluency. Images were captured every hour for a total of 60 h. Cells were incubated with or without 100 ng/ml of *Eschericia coli*-derived recombinant mouse IL-17A (R & D Systems).

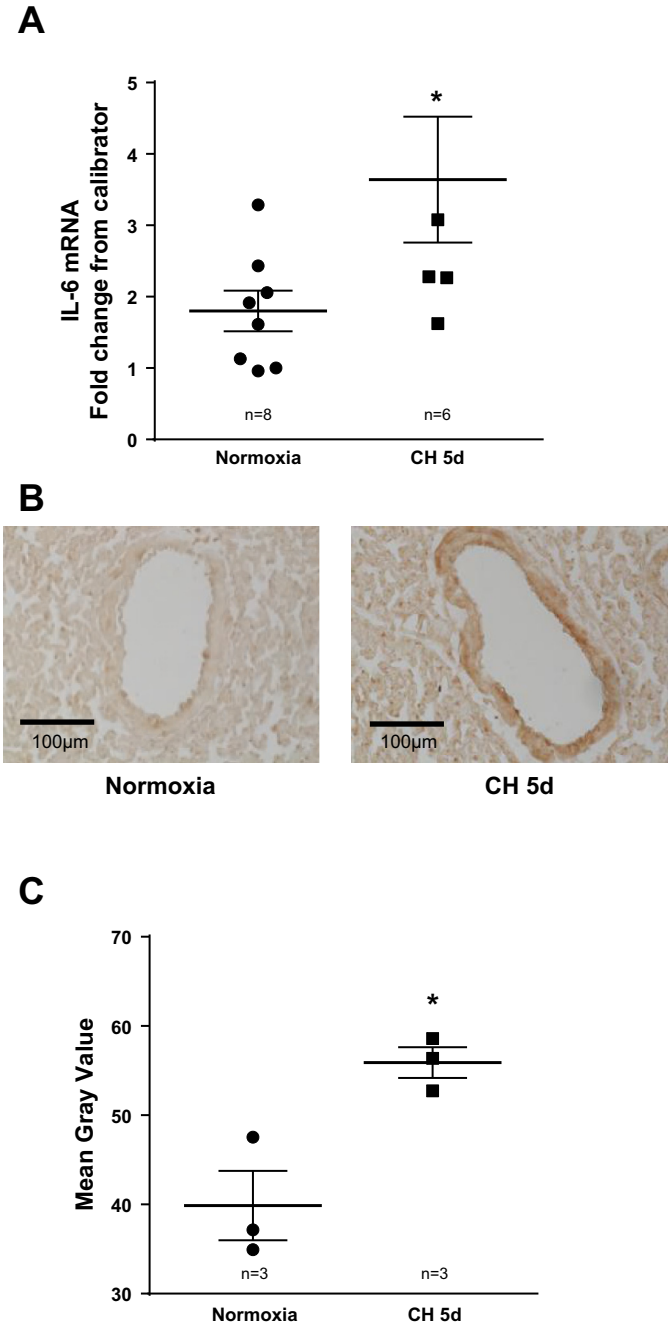

Fig. 3. CH increases lung IL-6 levels. *A*: lungs from mice exposed to either normoxia or 5 days of CH (CH 5d) were homogenized and IL-6 mRNA levels determined by real-time PCR, with β-actin used as an endogenous control. *B*: representative images of immunohistochemical detection of IL-6 in lung sections. *C*: summary analysis data of the mean gray value of the medial layer of anti-IL-6-stained pulmonary artery sections with external diameters of 30–80 μm. Values are means ± SE. *$P < 0.05$ vs. normoxia; $n = 3$ mice/group, 5–12 arteries/mouse, analyzed by unpaired *t*-test. ●, Normoxia; ■, chronic hypoxia.

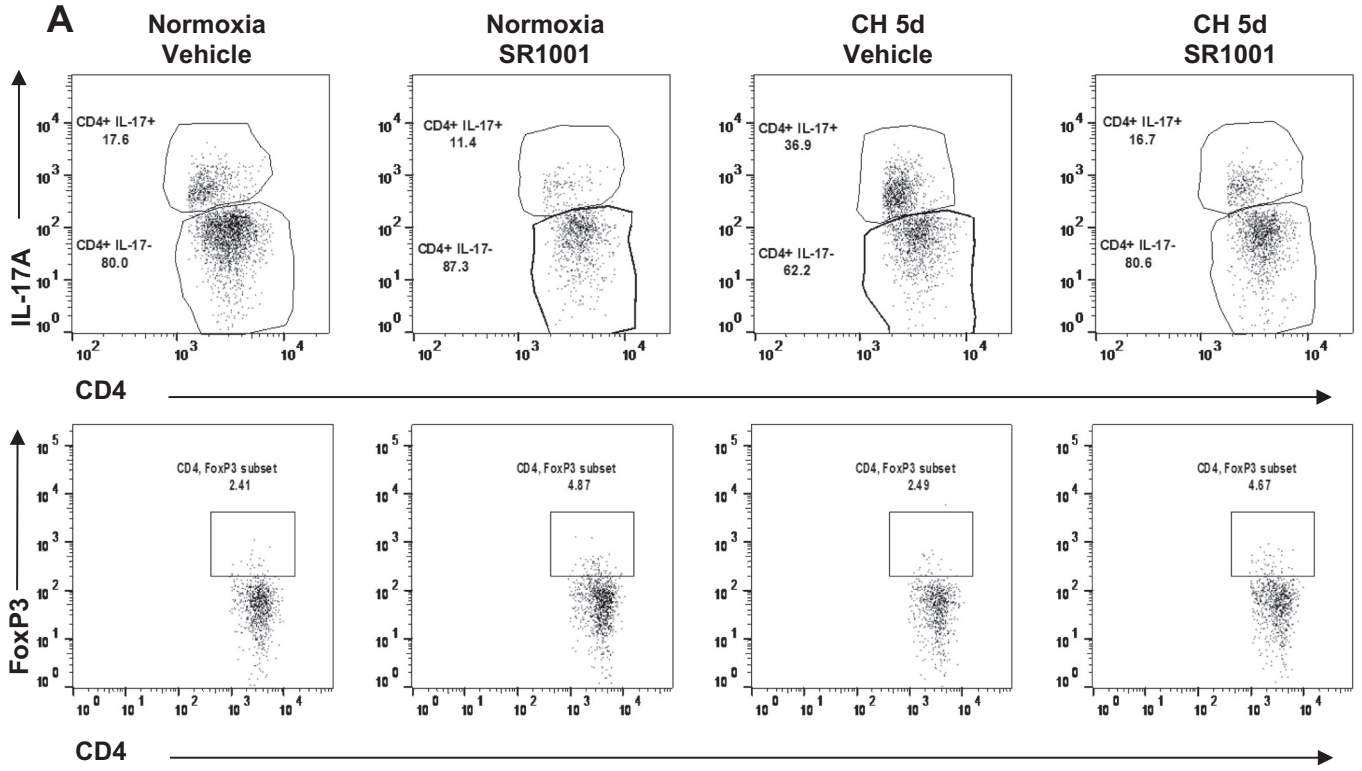

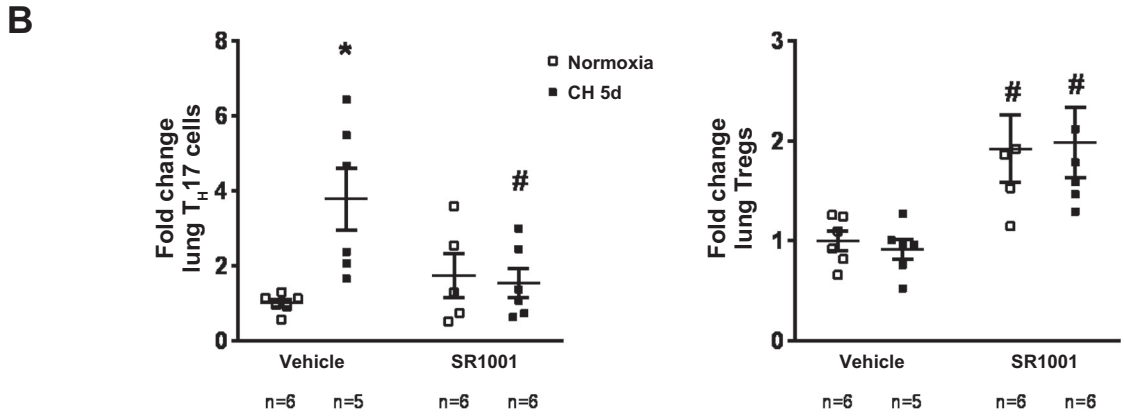

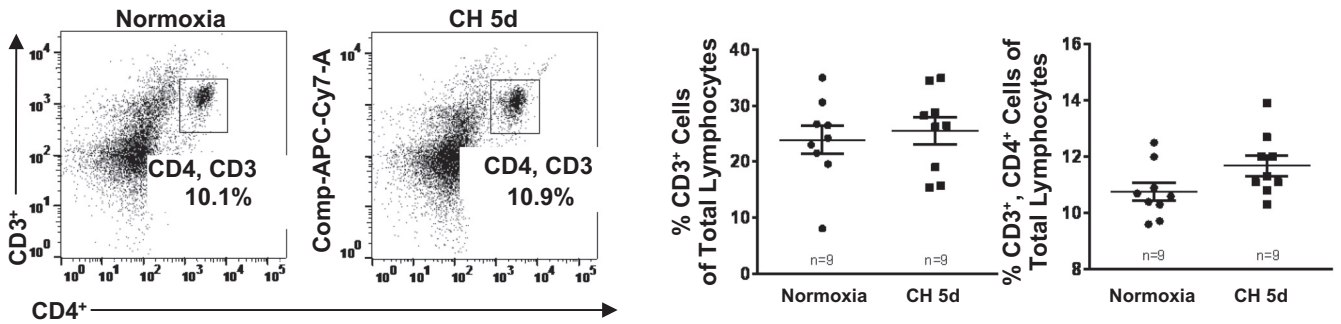

RT-PCR. Total lung RNA was extracted using Direct-zol (Zymo Research) and reverse transcribed to cDNA using the High-Capacity cDNA Reverse Transcription Kit (Life Technologies). The Roche Universal Probe Library System was used for real-time detection of IL-6 (5′-gctaccaaactggatataatcagga, 3′-ccaggtagctatggtactccagaa, probe 6), IL-21 (5′-ccaggtagctatggtactccagaa, 3′-ccaggtagctatggtactccagaa, probe 100), Fizz1 (5′-ccctccactgtaacgaag actc, 3′-cacacccagtagcagtcatcc, probe 51), NOS2 (5′-ctccatgactcccagcaca, 3′-actctcttgcggaccatctc, probe 101), and ACTB as a reference gene (5′-ctaaggccaaccgtgaaaag, 3′-accagaggcatacagggaca, probe 64). The normalized gene expression method ($2^{-\Delta\Delta C_T}$) was used for relative quantification of gene expression, using pooled samples as the calibrator (46).

Statistics. Results were expressed as means ± SE. Statistical significance was tested at the 95% ($P < 0.05$) confidence level using an unpaired *t*-test or two-way ANOVA followed by Student-Newman-Keuls posttest.

RESULTS

$CD4^+$ T cells contribute to CH-induced pulmonary hypertension. To assess the contribution of T cells to CH-induced PH, we used recombination-activating gene 1-KO ($RAG1^{-/-}$) mice, which lack mature T and B cells (35). $RAG1^{-/-}$ mice were exposed to CH or normoxia for 21 days. WT mice exhibited a significant increase in RVSP following CH (Fig. 1, *A* and *B*). However, this response to CH was attenuated largely in $RAG1^{-/-}$ mice that did not receive adoptive transfer or saline injection (No AT). Furthermore, adoptive transfer of $CD4^+$ T cells, but not $CD8^+$ T cells, was sufficient to restore the increased RVSP following CH (Fig. 1*B*). Similar results were observed for Fulton's index (Fig. 1*C*) and RV/body weight (Table 1). Adoptive transfer did not affect hematocrit, body weight, heart rate, or LV + S/body weight (Table 1).

CH significantly increased percent arterial wall thickness in WT mice, which was not present in $RAG1^{-/-}$ mice (Fig. 1, *D* and *E*). Adoptive transfer of $CD4^+$ but not $CD8^+$ T cells into $RAG1^{-/-}$ mice and subsequent exposure to CH demonstrated an increase in medial thickness similar to that observed in WT mice.

Adoptive transfer of either cell type did not affect any of the assessed parameters in normoxic mice (Fig. 1 and Table 1), indicating that the observed differences between groups were not due to the adoptive transfer per se but rather due to $CD4^+$ T cell restoration. As reported previously, responses to CH were not different between males and females (6).

We further tested the contribution of $CD4^+$ T cells to CH-induced PH by depleting $CD4^+$ cells using a CD4-neutralizing antibody. The efficacy of $CD4^+$ cell depletion is demonstrated by a reduction of $CD4^+$ T cells from 60 to 1% of total $CD3^+$ T cells in the spleen (Fig. 2*A*). As expected, WT mice receiving control antibody and exposed to CH for 21 days demonstrated an increase in RVSP, hematocrit, RV hypertrophy, and pulmonary arterial remodeling (Fig. 2, *B–E*). CD4 depletion prevented the CH-induced increase in RVSP and arterial wall thickness (Fig. 2, *B* and *D*). Although there was a blunted RV remodeling response to CH in $RAG1^{-/-}$ mice (Fig. 1*C*), this effect was statistically significant in $CD4^+$ cell-depleted mice (Fig. 2*C*). Body weight, heart rate, RV/body weight, LV + S/body weight (Table 2), and hematocrit (Fig. 2*E*) were also unaltered by CD4 depletion. These findings demonstrate that $CD4^+$ T cells contribute to CH-induced PH.

CH increases lung IL-6 levels. The development of T_H17 cells relies primarily on the presence of elevated levels of IL-6 (28). Therefore, we sought to examine lung IL-6 expression in normoxic and CH mice. Exposure of WT mice to 5 days of CH, a time previously reported to enhance IL-6 production (45), caused a significant increase in lung IL-6 mRNA levels (Fig. 3*A*). Furthermore, IL-6 immunostaining was greater in the medial layer of pulmonary arteries of mice exposed to 5 days of CH compared with normoxic controls (Fig. 3, *B* and *C*).

T_H17 cells but not Tregs are increased in the lung following CH. Studies show increased numbers of circulating T_H17 cells in patients with PAH (25) and COPD (56) and in lungs of CH-exposed mice (23). The proportion of Tregs among $CD4^+$ T cells is significantly higher in PAH patients than in controls (43), and Tregs suppress adaptive immune responses (1). However, it is currently unknown whether CH alters lung T_H17/Treg balance. Therefore, the percentage of $CD4^+$ $FoxP3^+$ cells relative to total $CD3^+$ T cells was determined concurrently with $CD4^+$ $IL\text{-}17A^+$ in lung digests of mice exposed to 5 days of CH or normoxia using flow cytometry. CH resulted in a fourfold increase in lung T_H17 cells (Fig. 4, *A* and *B*). No significant difference in the percentage of $CD4^-$ $IL\text{-}17A^+$ cells (data not shown) and $CD4^+$ $FoxP3^+$ (Fig. 4, *A* and *B*) relative to total $CD3^+$ T cells was detected in lungs between normoxia- and CH-exposed mice.

In addition, total lung $CD3^+$ and $CD3^+/CD4^+$ T cells were similar between normoxic and CH mice (Fig. 4, *C* and *D*).

T_H17 cell development depends on signaling from the nuclear receptors RORα and RORγτ (58). SR1001 inhibits these receptors and T_H17 cell development both in vitro and in vivo (49). To confirm this effect of SR1001 in our preparation, mice were treated with vehicle or SR1001 and exposed to CH for 5 days or left in normoxia, and lung T_H17 and Tregs were measured by flow cytometry. SR1001 significantly attenuated CH-induced increases in lung T_H17 cells, with no effect in normoxic mice (Fig. 4, *A* and *B*). In contrast, SR1001 significantly increased Tregs in both normoxic and CH-exposed mice (Fig. 4, *A* and *B*).

To determine whether the increase in lung T_H17 cells is localized to the perivascular region, mice were treated with SR1001 and exposed to CH for 2, 5, or 21 days. T cells were examined in lung sections by immunohistochemical detection of the pan-T cell marker CD3. CH increased the incidence of

Fig. 4. CH leads to an increase in lung T helper 17 (T_H17) cells without T regulatory cells being affected. Lungs were removed from vehicle- and SR1001 (25 $mg \cdot kg^{-1} \cdot day\ sc^{-1}$)-treated mice after 5 days of normoxic or CH (CH 5d) exposure. Single-cell suspensions from the lungs were labeled with anti-CD3, anti-CD4, and anti-IL-17A or FoxP3. *A*: representative scatter plots. Cells were gated based on forward and side scatter and CD3 CD4. *B*: summary of the $\%CD4^+$ $IL\text{-}17A^+$ or $CD4^+$ $FoxP3^+$ cells relative to total $CD3^+$ cells normalized to the average of the vehicle-treated normoxic group of each set of experiments. *C*: representative scatter plots of $CD3^+$, $CD4^+$ T helper cells from lungs from mice exposed to normoxia or 5 days of CH. *D*: summary of the $\%CD3^+$ T cells relative to total cells and $CD3^+$, $CD4^+$, and T helper cells relative to total $CD3^+$ cells. Values are means ± SE; *n* = no. of animals, $*P < 0.05$ vs. normoxia vehicle; $\#P < 0.05$ vs. CH vehicle, analyzed by 2-way ANOVA, followed by multiple-comparison Student-Newman-Keuls test.

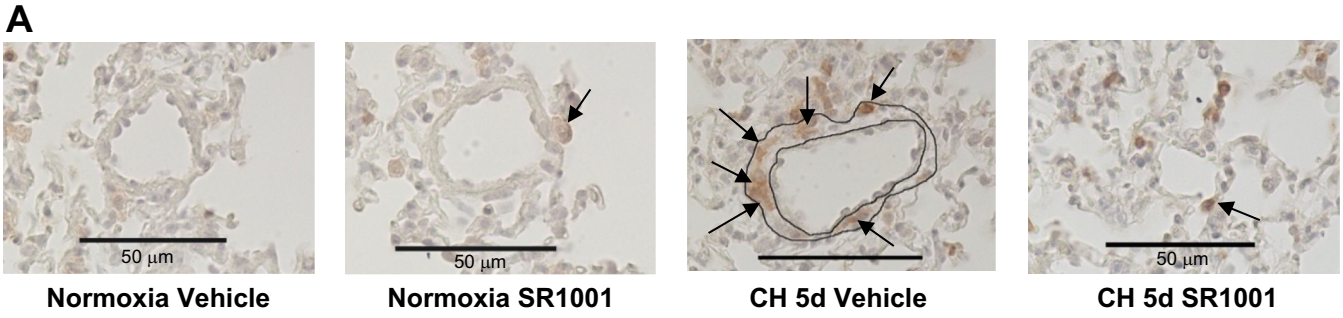

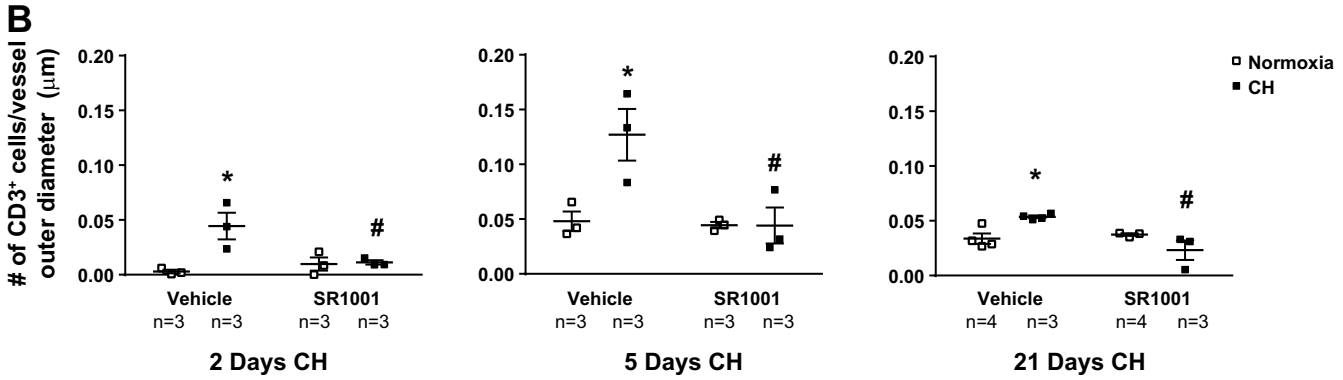

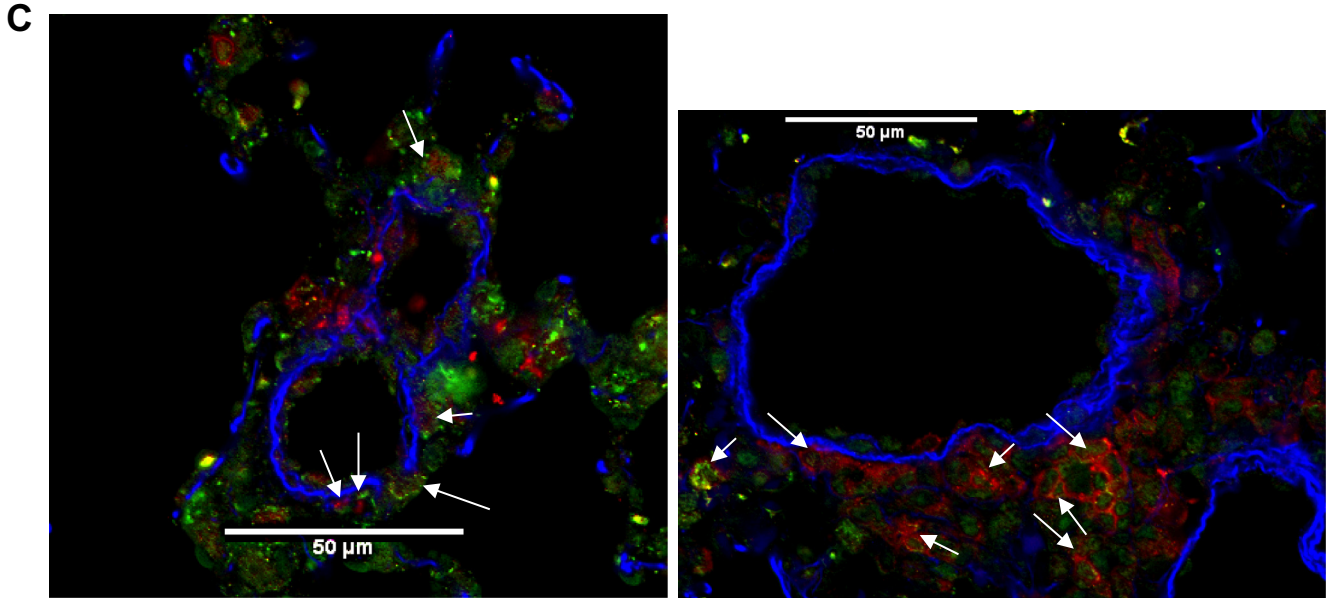

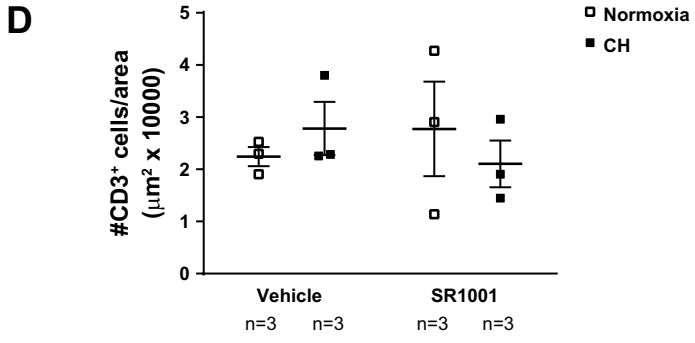

$CD3^+$ T cells in the pulmonary arterial perivascular region of vehicle-treated mice (Fig. 5, *A* and *B*). SR1001 prevented this response to CH at all three time points (Fig. 5, *A* and *B*). The majority of perivascular $CD3^+$ cells were found to be IL-$17A^+$ in arteries from CH mice (Fig. 5*C*). The increase in perivascular T cells following CH was not due to an increase in total lung T cells (Fig. 4*C*). Furthermore, SR1001 did not affect T cell density in the in lung parenchyma (Fig. 5*D*).

T_H17 cells contribute to CH-induced PH. SR1001 administration attenuated CH-induced increases in RVSP, RV hypertrophy, pulmonary arterial remodeling, and Ki-67^+ (proliferation marker) cells in the walls of small pulmonary arteries without affecting the polycythemic response (Fig. 6). No apoptotic cells were detected in pulmonary arteries from any of the groups (Fig. 6*F*).

To further confirm a role for T_H17 cells in CH-induced PH, in vitro-polarized T_H17 cells were administered to $RAG1^{-/-}$ mice exposed to CH or normoxia. Mice receiving T_H17 cells developed an increase in RVSP along with pulmonary arterial remodeling independent of normoxic or CH exposure (Fig. 7, *A* and *B*). Interestingly, RV remodeling did not develop in normoxic mice receiving adoptive transfer (Fig. 7*C*) despite evidence of PH. Rather, both RV/body weight and LV + S/body weight were significantly lower in normoxic $RAG1^{-/-}$ mice that received adoptive transfer of T_H17 cells compared with those not receiving adoptive transfer (Table 3). This effect was not due to a decrease in body weight (Table 3). The polycythemic response to CH was not affected by adoptive transfer of T_H17 cells (Fig. 7*D*). Successful adoptive transfer was demonstrated by $CD3^+$ T cell labeling in lung sections from adoptively transferred mice but not in sham (saline)-treated mice (Fig. 7*E*). $CD4^+$ $EGFP^+$ cells were also found in the spleen by flow cytometry (Fig. 7*F*).

T_H17 cell inhibition lowers RVSP in established PH. We sought to understand whether CH-induced PH can be reversed once already established by inhibiting T_H17 cell development. Consistent with this possibility, SR1001 significantly lowered RVSP (Fig. 8*A*). A trend for decreased RV hypertrophy ($P < 0.0583$) and pulmonary arterial remodeling ($P < 0.20$) was also observed (Figs. 8, *B* and *C*). SR1001 decreased the number of perivascular T cells (Fig. 8*D*).

IL-17A increases mouse PASMC migration. Controversy exists as to whether T_H17 cells can have a direct effect on tissue through the release of T_H17-associated cytokines (23, 30) or indirectly by recruiting neutrophils and/or macrophages (31). To determine whether macrophages are implicated in the pathogenesis of PH in our experimental conditions, total macrophage numbers were determined by flow cytometry in lungs of vehicle- and SR1001-treated mice exposed to normoxia or 5 days of CH. No significant difference in the percentage of $F4/80^+$ $CD11b^+$ cells relative to total $CD45^+$ cells was detected between groups (Fig. 9, *A* and *B*). IL-21 transcript levels were additionally measured in the lungs of mice exposed to normoxia or 5 days of CH together with mRNA levels of the M2 marker Fizz1 and the M1 marker NOS2. No significant differences in IL-21, Fizz1, or NOS2 mRNA levels were found between groups (Fig. 10). Furthermore, IL-17A increased mouse PASMC migration as assessed using a scratch wound-healing assay (Fig. 11*A*) but had no effect on cell culture confluency (Fig. 11*B*).

DISCUSSION

In both humans and rodents, alveolar hypoxia results in an inflammatory phenotype in the lung (9, 19, 20, 24, 33, 50). Inflammation occurs before morphological changes in the vasculature, suggesting that lung hypoxia may lead to damaging inflammatory effects (20). Release of cytokines and chemokines from inflamed tissues may contribute to differentiation of naïve T cells into mature effector T cells and their migration to the site of inflammation. However, the contribution of T helper subsets to the pathogenesis of hypoxic PH is not clear, and the mechanism and specific inflammatory cell types involved are not well defined. Our study shows that $CD4^+$ T cells, specifically T_H17 cells, contribute to CH-induced PH, and their presence in the perivascular space likely contributes to this disease.

Cuttica et. al (13) reported that $RAG1^{-/-}$ mice are protected from monocrotaline-induced PAH and that $CD4^+$ T cells are the primary effector cells. However, the role for $CD4^+$ T cells in PH due to CH has not been assessed directly. For the first time, our study demonstrates that $CD4^+$ T cells are both necessary and sufficient for a robust pulmonary-hypertensive response to CH. In addition, our study suggests that $CD8^+$ T cells might not contribute to CH-induced PH because immune reconstitution of $RAG1^{-/-}$ mice with $CD8^+$ T cells did not affect the already attenuated response of these mice to CH. Furthermore, our data suggest that B cells are not major contributors to the pathogenesis of PH since $CD4^+$ T cells' reconstitution fully restored the pulmonary-hypertensive response to CH in $RAG1^{-/-}$ mice and $CD4^+$ T cells' depletion attenuated it. Further supporting a minimal role for B cells, in an initial pilot study, adoptive transfer of splenocytes from a T cell receptor knockout mouse (lacks all mature T cells but has B cells) failed to restore the PH response in $RAG1^{-/-}$ mice (data not shown).

Inflammation in rat pulmonary arteries after CH exposure has been characterized by increased numbers of monocytes and dendritic cells, with few T cells and no B cells (9). Conversely, in monocrotaline-treated mice, perivascular infiltration largely

Fig. 5. Inhibition of T_H17 cell development attenuates CH-induced increases in perivascular T cells. SR1001 was delivered daily by sc injection (25 $mg \cdot kg^{-1} \cdot day^{-1}$) for the duration of normoxic or CH exposure. *A*: representative images from normoxic and CH (5 days) mice treated with or without SR1001 in which perivascular T cells ($CD3^+$ cells) were quantified. Arrows depict $CD3^+$ cells. Scale bar, 100 μm. *B*: summary of the no. of perivascular $CD3^+$ cells from mice exposed to 2, 5, or 21 days of normoxia or CH treated with or without SR1001. The perivascular region was defined as external to vessel media and internal to vessel adventitia. *C*: representative images of lung sections from vehicle-treated mice exposed to 21 days of CH colabeled with anti-IL17A (green) and anti-CD3 (red). Elastic lamina is shown in blue. Arrows depict double-positive cells. Scale bar, 50 μm. *D*: summary of the no. of $CD3^+$ cells in the lung parenchyma of mice exposed to 5 days of normoxia or CH treated with or without SR1001. Values are means ± SE. $*P < 0.05$ vs. normoxia vehicle; $\#P < 0.05$ vs. vehicle CH; n = no. of animals; at least 5–15 arteries (<150 μm outer diameter/mouse) were measured and analyzed by 2-way ANOVA, followed by multiple comparisons Student-Newman-Keuls test.

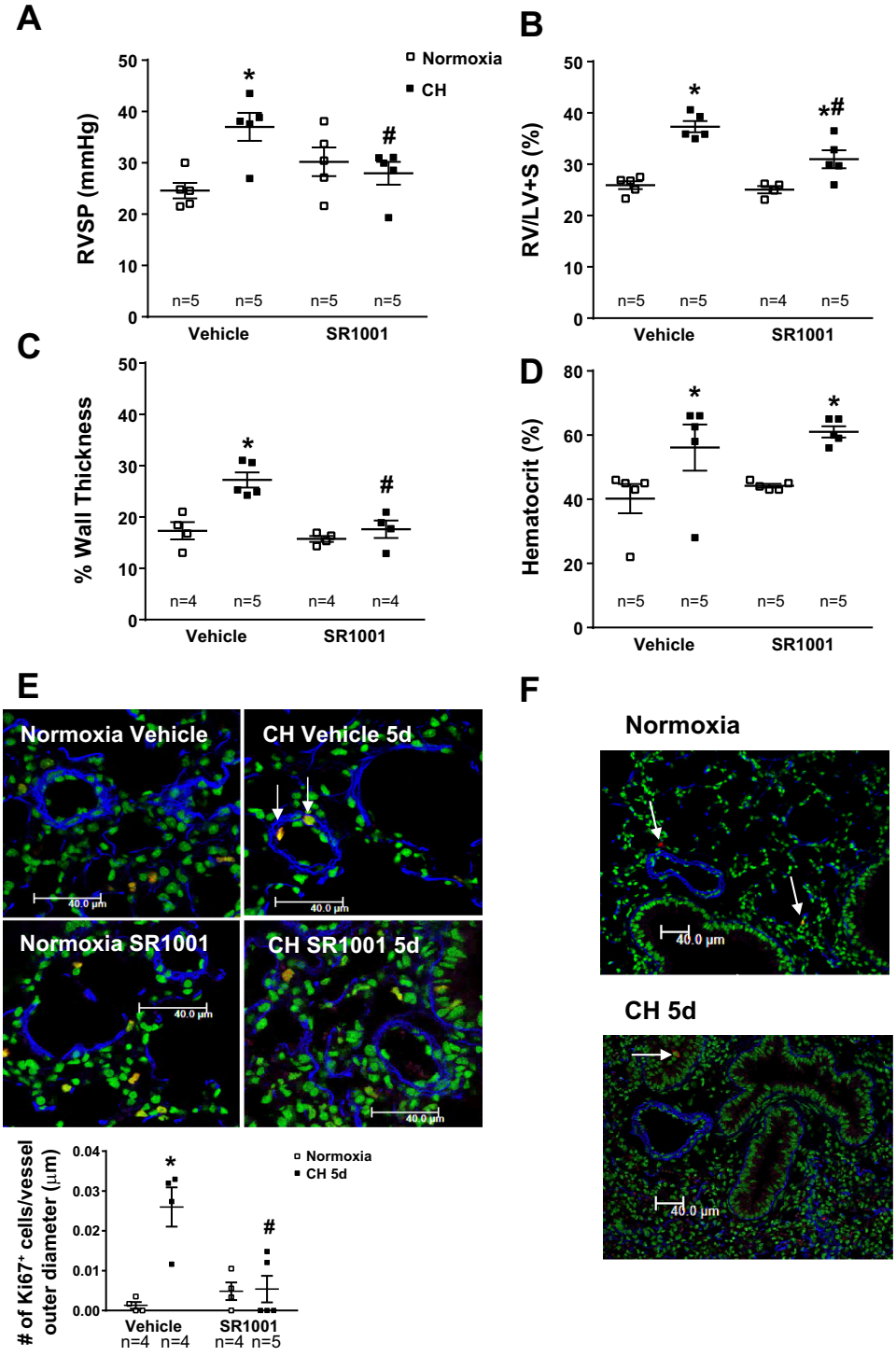

Fig. 6. Inhibition of T_H17 cell development attenuates CH-induced PH. SR1001 was delivered sc (25 mg·kg^{-1}·day^{-1}) via an implantable osmotic pump. *A*: RVSP following 21 days of normoxia or CH. *B*: Fulton's index. *C*: pulmonary arterial wall thickness measured in small pulmonary arteries (<150 μm) labeled for α-smooth muscle actin. *D*: hematocrit. *E*: no. of Ki-67$^+$ cells/small pulmonary artery outer diameter. Ki-67 is a marker of cell proliferation. Ki-67$^+$ cells were detected by immunofluorescence microscopy in the arterial wall (shown in red). The elastic lamina in the arterial wall is shown in blue. Nuclei are shown in green. CH 5d, 5 days of CH. *F*: representative images of lung sections labeled with anti-cleaved caspase 3, which is an apoptosis marker. Scale bar, 40 μm. Arrows depict positive cells expressing activated caspase 3 in lung parenchyma. Values are means ± SE; n = no. of animals, and in *C* and *D* at least 10 arteries/animal were measured. *P < 0.05 vs. normoxia vehicle; #P < 0.05 vs. normoxic SR1001, analyzed by 2-way ANOVA, followed by multiple-comparison Student-Newman-Keuls test.

involves CD4$^+$ T cells along with fewer macrophages and B cells (13). However, the subset of CD4$^+$ T cells involved in the pathogenesis of PH or PAH is not clear.

T_H17 cells are important mediators of tissue damage in immune-mediated inflammatory diseases such as asthma, inflammatory bowel disease (55), and cardiovascular diseases (11, 18), including systemic hypertension (32). T_H17 cells act by attracting neutrophils and stimulating the release of matrix metalloproteinases as well as increasing the release of factors from resident cells (31). The development of T_H17 cells relies primarily on the presence of elevated levels of IL-6 (28, 29). Increased numbers of circulating T_H17 cells have been reported in COPD (56) and PAH patients (25). Hasimoto-Kataoka et. al (23) have recently shown an effect of CH (3 days) to increase lung T_H17 cell numbers in mice, which was prevented by administration of an anti-IL-6 receptor antibody. However, these previous studies have addressed neither where these cells accumulate in the lungs nor their contribution to PH.

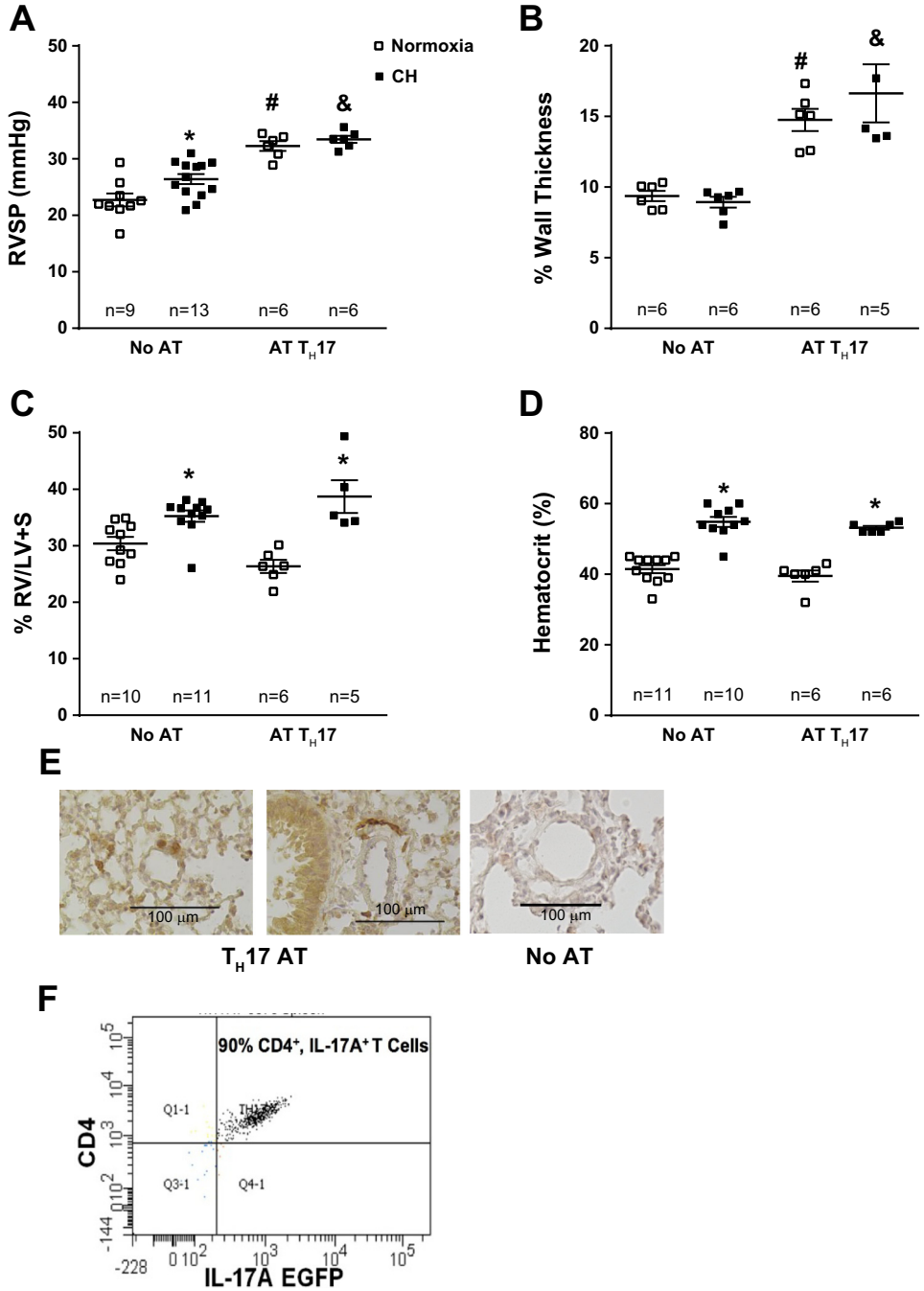

Fig. 7. The adoptive transfer of T_H17 cells causes spontaneous PH in RAG1$^{-/-}$ mice. CD4$^+$ T cells were purified from IL-17A enhanced green fluorescent protein (EGFP) mice and cultured under T_H17-polarizing conditions. T_H17 cells were purified by fluorescence-activated cell sorting and injected into RAG1$^{-/-}$ mice. After 14 days, mice remained in normoxia or were exposed to CH for 21 days and compared with mice that did not receive T_H17 cells. *A*: RVSP. *B*: %wall thickness. *C*: Fulton's index. *D*: hematocrit. *E*: representative images of lung sections immunostained for CD3 from mice receiving adoptive transfer or a RAG1$^{-/-}$ mouse that received no adoptive transfer. Scale bars, 100 μm. *F*: flow cytometric analysis of T_H17 cells from the spleens of mice that received an adoptive transfer. Values are means ± SE; n = no. of animals. $^*P < 0.05$ vs. normoxia; $^\#P < 0.05$ vs. normoxia No AT; $^\&P < 0.05$ vs. CH No AT. Analyzed by 2-way ANOVA, followed by multiple comparisons Student-Newman-Keuls test.

Our results demonstrate that CH increases the proportion of T_H17 cells without affecting the proportion of Tregs or total T cell numbers in the lungs and that increased T_H17 cells are localized in the perivascular region of small pulmonary arteries. The increase in T_H17 cells was associated with increased lung IL-6 mRNA and peptide levels in the medial layer of pulmonary arteries. These results showing increased lung IL-6 expression in response to CH are consistent with previous reports demonstrating that IL-6 plays a critical role in the development of PH (23, 45). Although IL-6 inhibits TGFβ-induced Treg differentiation (28), our results suggest that in CH the balance of T_H17/Treg is altered in the lung due to an increase in T_H17 cells but not due to changes in Tregs. However, these findings do not preclude the possibility that Treg numbers are altered at different exposure times. In addition, the decreased proportion of Tregs in the lungs could have affected the pathogenesis of PH since it has been shown that adoptive transfer of Tregs into WT mice prevents CH-induced PH (12).

Our study demonstrates a novel effect of a T_H17 inhibitor, SR1001, to attenuate the development of CH-induced PH. Furthermore, mice that received adoptive transfer of T_H17 cells under normoxic conditions developed spontaneous increases in RVSP and pulmonary arterial remodeling. Thus, our data strongly support a pathogenic role of T_H17 cells in the development of PH.

Table 3. *Biometrics of RAG1$^{-/-}$ mice exposed to normoxia or CH with or without the adoptive transfer of T_H17 cells*

Treatment	Exposure	HR beats/min	Hto, %	BW, g	LV + S/BW, mg/g	RV/BW, mg/g	*n* (mice)	*n* (females)
No AT	Normoxia	377 ± 23	42 ± 2	28.1 ± 1.3	3.39 ± 0.08	0.92 ± 0.04	6	3
No AT	CH	413 ± 10	51 ± 3*	24.6 ± 1.3*	3.46 ± 0.10	1.20 ± 0.10*	6	3
T_H17 AT	Normoxia	423 ± 12	40 ± 2	26.0 ± 0.3	3.02 ± 0.06†	0.80 ± 0.04†	6	3
T_H17 AT	CH	415 ± 19	53 ± 1*	22.1 ± 1.2*	3.14 ± 0.09	1.19 ± 0.05*	6	3

Values are means ± SE. T_H17, T helper 17; WT, wild-type; AT, adoptive transfer; HR, heart rate; Hto, hematocrit; BW, body weight; LV + S, left ventricle + septum; RV, right ventricle; CH, chronic hypoxia. *$P < 0.05$ vs. normoxia; †$P < 0.05$ vs. no AT normoxia.

Interestingly, we found that lungs of mice that received the adoptive transfer of T_H17 cells under normoxic conditions displayed a remarkable increase in the number of CD3$^+$ T cells in both the parenchymal and perivascular regions. These data suggest that polarizing naïve CD4$^+$ T cells to T_H17 cells ex vivo mimics conditions occurring in the lung in response to CH.

It is possible that ROR$\gamma\tau^+$ innate lymphoid cells (2) contribute to CH-induced PH. However, this possibility is unlikely because *1*) no significant increase in CD3$^+$ CD4$^-$ IL-17A$^+$ cells was detected by flow cytometry in the lungs of mice exposed to CH compared with controls, *2*) CD4$^+$ T cell-replete RAG1$^{-/-}$ mice developed PH in response to CH, *3*) normoxic mice that received T_H17 cells displayed evidence of PH, and *4*) most CD3$^+$ T cells present in the perivascular region were IL-17A$^+$ cells.

A dissociation between RVSP and RV remodeling was observed in CD4$^+$ cell-depleted (Fig. 3) and T_H17 cell-replete mice (Fig. 8). Although it has been widely believed that sustained pressure overload is sufficient to result in adaptive hypertrophy of the heart, this and other studies (3, 16, 41, 51) suggest that hypoxia itself is a major contributor to RV remodeling through mechanisms that are partially independent of pressure overload. The mechanism that underlies the dissociation between RVSP and RV remodeling is currently unknown.

The heart weight of mice that received adoptive transfer of T_H17 cells under normoxic conditions was lower than that of control mice. These mice appeared healthy in that they did not show indications of colitis, and their weight remained relatively stable. Therefore, the decrease in heart weight cannot be explained by a general state of stress induced by a systemic inflammatory reaction. The reason of the decrease in heart weight is currently unknown and requires further investigation.

To follow up on the immunological timing of events, we sought to understand whether PH due to CH might be reversed by inhibition of T_H17 cell polarization. We demonstrated that established PH markers such as increased RVSP can be reduced by treating animals with SR1001. We observed a strong tendency for a reduction in RV remodeling and a significant decrease in perivascular T cell infiltration. The reversal of fixed components (remodeling) of PH might require longer treat-

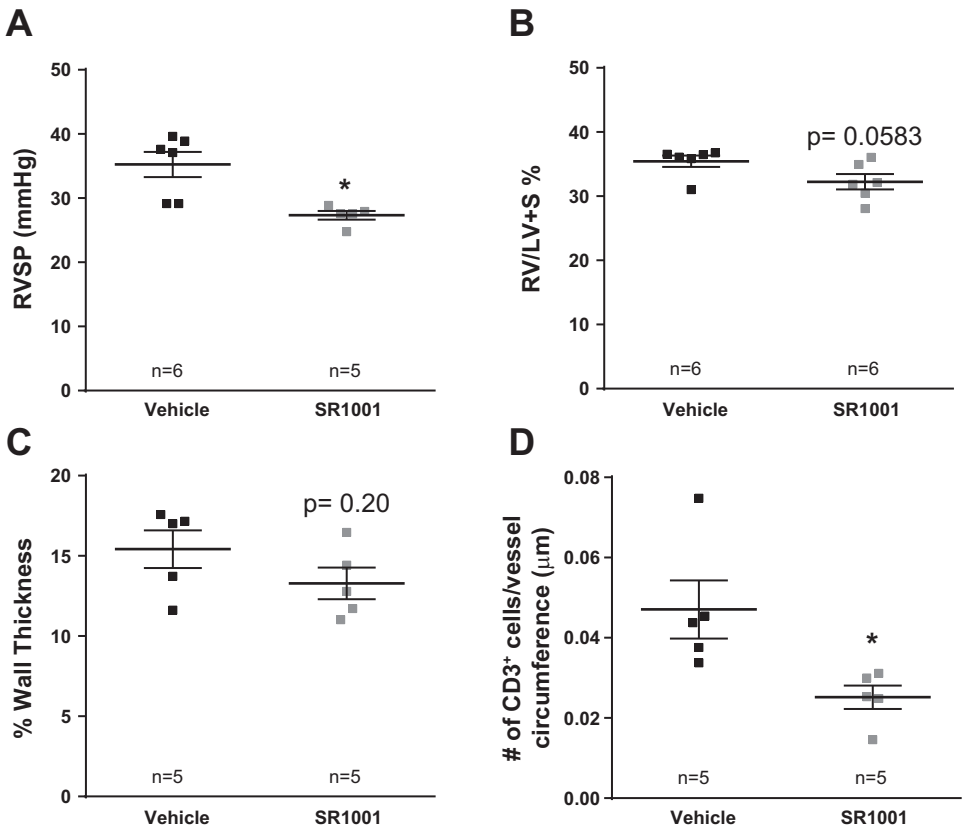

Fig. 8. Inhibition of T_H17 cell polarization reverses CH-induced PH. Wild-type mice were exposed to CH for 21 days, followed by administration of SR1001 (25 mg·kg^{-1}·day sc^{-1}) or vehicle for an additional 14 days in CH. *A*: RVSP. *B*: Fulton's index. *C*: %wall thickness. *D*: no. of CD3$^+$ cells/vessel diameter (μm). Values are means ± SE; *n* = no. of animals, and in *C* and *D* at least 10 arteries/animal were measured. *$P < 0.05$ vs. vehicle, analyzed by unpaired *t*-test.

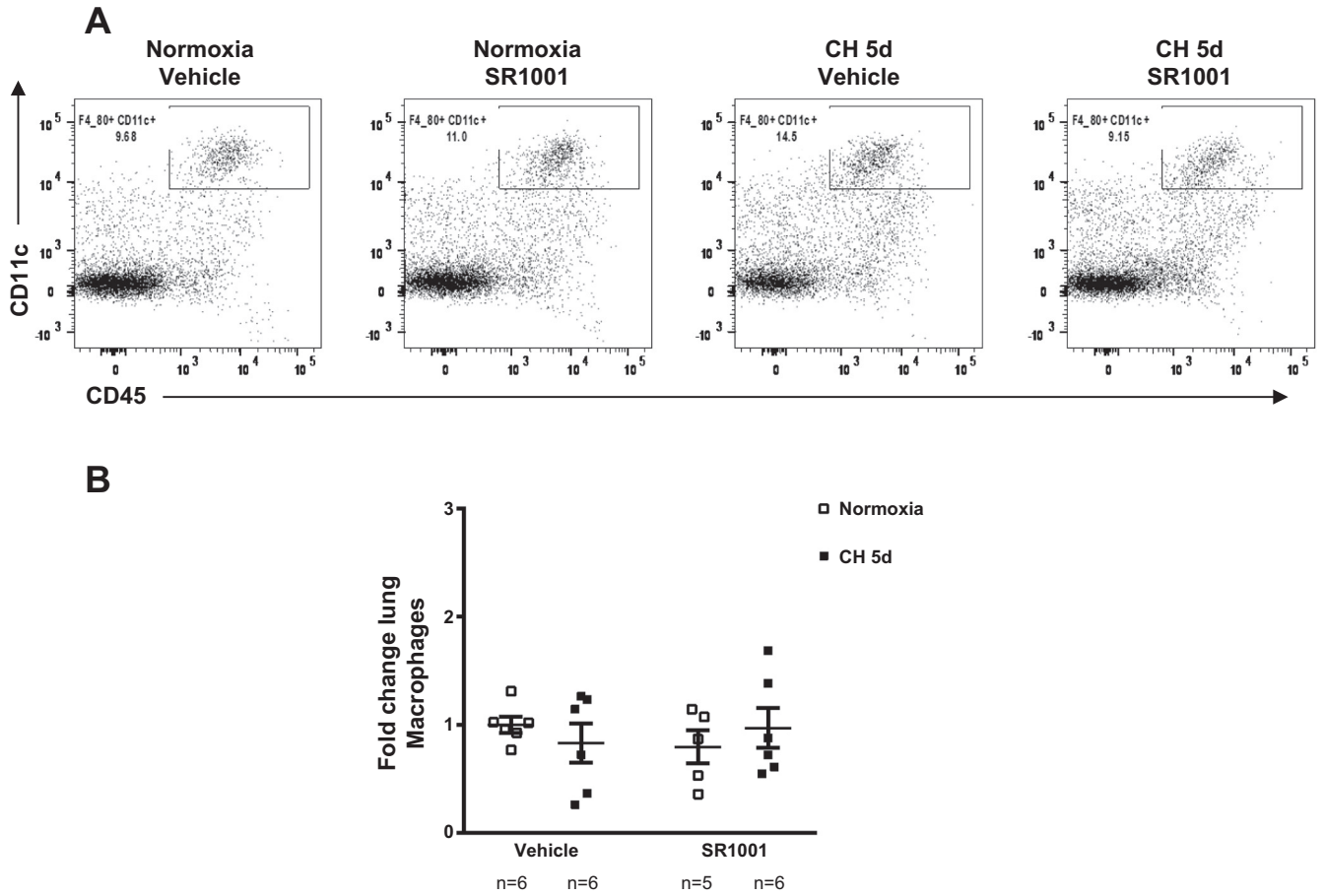

Fig. 9. Total lung macrophage numbers are not affected by CH exposure. Lungs were removed from mice following 5 days of CH exposure. Single-cell suspensions from the lungs were incubated with anti-CD45, anti-F4/80, and anti-CD11b to label macrophages. *A*: representative scatter plots. Cells were gated based on forward and side scatter and CD45. *B*: summary of %F4/80$^+$ CD11c$^+$ cells relative to total CD45$^+$ cells normalized to the average of the vehicle-treated normoxic group of each set of experiments. Values are means ± SE; n = no. of animals, analyzed by 2-way ANOVA, followed by multiple-comparison Student-Newman-Keuls test.

ment. It has been demonstrated previously that SR1001 prevents the polarization of naïve CD4$^+$ T cells to T_H17 cells and significantly delays the onset of T_H17 cell-mediated experimental autoimmune encephalomyelitis in mice and reduces disease severity (49). This is similar to our results in which SR1001 was more effective if given earlier in disease progression rather than if after disease is well established. Our data indicate that significant perivascular T cell infiltration persists after 21 days of CH. Therefore, it is likely that there is an initial contribution of CH to the polarization of naïve CD4$^+$ T cells, which establishes disease, but long-standing, lower levels of chronic inflammation may help sustain CH-induced PH.

Contrary to the report by Solt et. al. (49) showing that SR1001 has no effect on Treg development in vitro, but consistent with in vivo studies (7, 48), here we show that SR1001 increases lung Tregs, suggesting an additional mechanism by which SR1001 could have prevented and reversed CH-induced PH (12). However, several lines of evidence support T_H17 cells as the major effector inflammatory cells following CH, including the following: *1*) the majority of perivascular T cells were IL-17A$^+$ cells; *2*) SR1001 did not affect the number of perivascular CD3$^+$ T cells in normoxic mice while preventing CH-induced perivascular inflammation; and *3*) CH did not increase lung Tregs. Further studies exploring the mechanism by which ROR inhibitors alter T_H17/Treg balance are warranted.

T_H17 cells are characterized by the predominant production of IL-17A (4). We found that IL-17A enhanced PASMC migration but did not affect cell number or confluency. These results are consistent with a report showing that IL-17A promotes migration of airway smooth muscle cells (10) but contrary to a report showing that it enhances fibroblast proliferation (17). Therefore, our results suggest that IL-17A produced by T_H17 cells plays an important role in the pathogenesis of CH-induced PH. It has been reported that T_H17 cells promote M2 macrophage polarization through the release of IL-21 (23); however, we did not find a significant change in lung macrophage infiltration, IL-21 mRNA, or expression of M2 or M1 markers in response to CH. A few differences in experimental design could explain the discrepancy between studies. For example, the earlier study used normobaric hypoxia with no CO_2 supplementation, and whereas we used hypobaric hypoxia, they determined these markers in bronchoalveolar lavage while we used whole lung, and although we both used C57B6 mice, the mice were from different sources. Regardless, further studies are warranted to establish the mechanism of T_H17 cell-mediated PH pathogenesis.

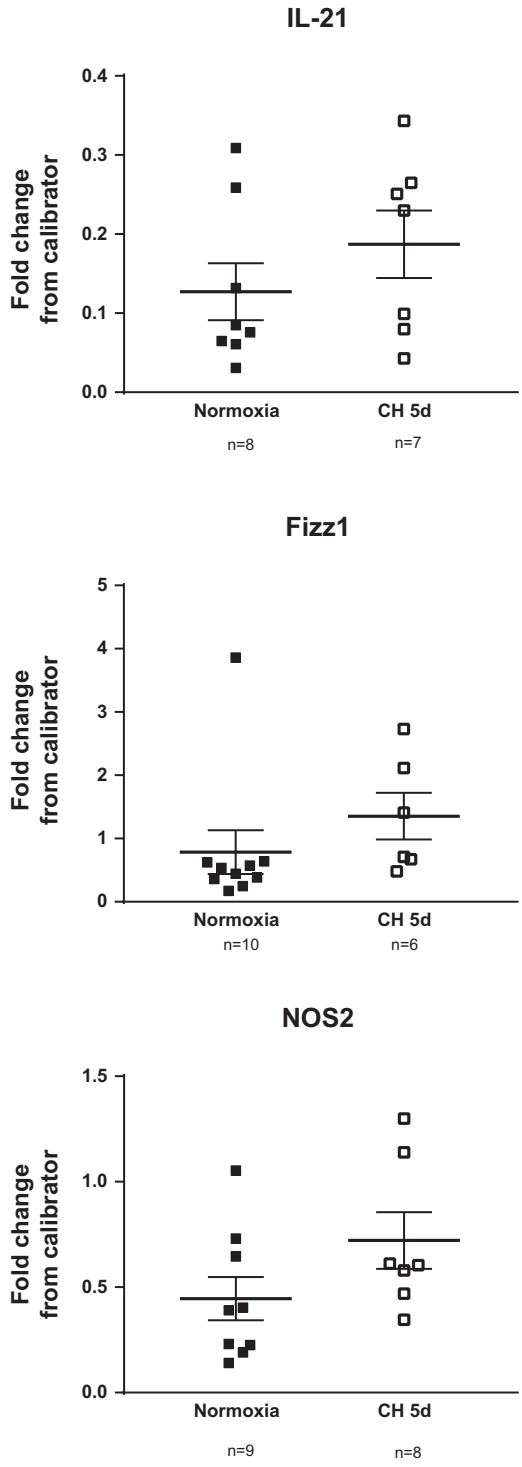

Fig. 10. CH does not affect lung IL-21, Fizz1, or NOS2 mRNA levels. IL-21, Fizz1 (macrophage type 2 marker), and NOS2 (macrophage type 1 marker) transcripts were measured by real-time PCR in lungs from WT mice exposed to normoxia or 5 days of CH. Values are means ± SE; n = no. of animals, analyzed by unpaired t-test.

In summary, this study directly demonstrates a causal link between $CD4^+$ T cells and PH under hypoxic conditions, specifically pointing to T_H17 cells. It also demonstrates that CH increases perivascular T cell localization, a response that is prevented by an inhibitor of RORγτ, the signature nuclear receptor for T_H17 cells. Furthermore, our findings suggest that inhibition of T_H17 cell development may provide a novel therapeutic approach to treat pulmonary-hypertensive patients.

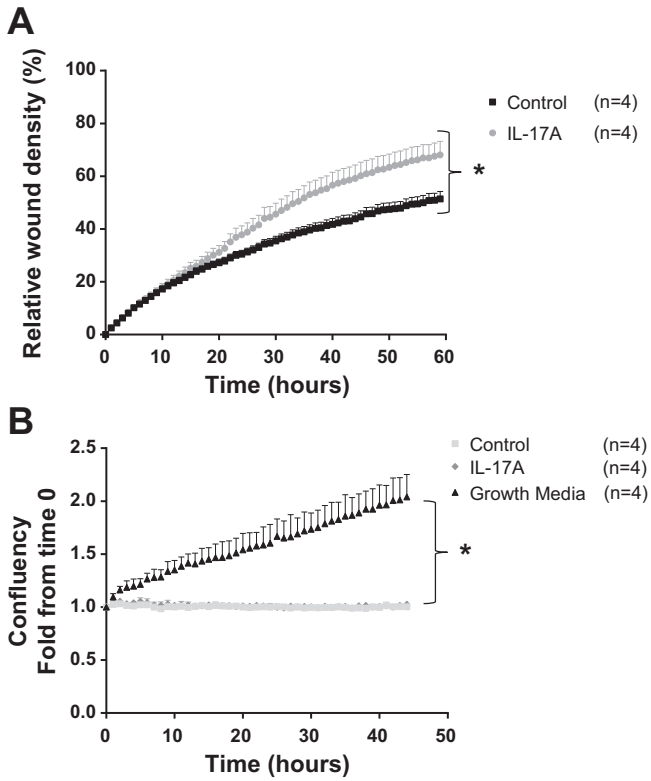

Fig. 11. IL-17A stimulates migration but does not affect mouse pulmonary arterial smooth muscle cell number in culture. *A*: %wound density in the presence or absence of IL-17A (100 ng/ml). *B*: confluency density normalized to *time 0* in the presence or absence of IL-17A (100 ng/ml) in serum-starved cells. Growth medium was used a positive control. *$P < 0.05$, cells from n = 4 mice, 2-way repeated-measures ANOVA, followed by multiple-comparison Student-Newman-Keuls test.

ACKNOWLEDGMENTS

We thank Eliseo Castillo for technical advice. Some of the images in this paper were aquired in the University of New Mexico & Cancer Center Fluorescence Microscopy Shared Resource and funded as detailed at the following link: http://hsc.unm.edu/crtc/microscopy/acknowledgement.shtml.

GRANTS

This study was supported by Grants F30-HL-123109 [National Heart, Lung, and Blood Institute(NHLBI)] to L. D. Maston, AHA 15GRNT25090038 to L. V. Gonzalez Bosc, T32-HL-007736, R01-HL-88192 (both NHLBI), and AHA 13GRNT14510041 to T. C. Resta, R01-AI-097202 to J. L. Cannon, and NSF CHE-1565085 to W. Wang.

DISCLOSURES

No conflicts of interest, financial or otherwise are declared by the authors.

AUTHOR CONTRIBUTIONS

L.D.M., J.L.C., T.C.R., and L.V.G.B. conceived and designed research; L.D.M., D.T.J., W.G., T.A.H., W.W., Y.W., W.X., and L.V.G.B. performed experiments; L.D.M., D.T.J., W.G., T.A.H., and L.V.G.B. analyzed data; L.D.M., W.G., J.L.C., T.C.R., and L.V.G.B. interpreted results of experiments; L.D.M. and L.V.G.B. prepared figures; L.D.M., T.C.R., and L.V.G.B. drafted manuscript; L.D.M., J.L.C., T.C.R., and L.V.G.B. edited and revised manuscript; L.D.M., D.T.J., W.G., T.A.H., J.L.C., W.W., Y.W., W.X., T.C.R., and L.V.G.B. approved final version of manuscript.

REFERENCES

1. **Akdis CA, Akdis M.** Mechanisms and treatment of allergic disease in the big picture of regulatory T cells. *J Allergy Clin Immunol* 123: 735–746, 2009. doi:10.1016/j.jaci.2009.02.030.
2. **Artis D, Spits H.** The biology of innate lymphoid cells. *Nature* 517: 293–301, 2015. doi:10.1038/nature14189.
3. **Ball MK, Waypa GB, Mungai PT, Nielsen JM, Czech L, Dudley VJ, Beussink L, Dettman RW, Berkelhamer SK, Steinhorn RH, Shah SJ, Schumacker PT.** Regulation of hypoxia-induced pulmonary hypertension by vascular smooth muscle hypoxia-inducible factor-1α. *Am J Respir Crit Care Med* 189: 314–324, 2014. doi:10.1164/rccm.201302-0302OC.
4. **Bettelli E, Korn T, Oukka M, Kuchroo VK.** Induction and effector functions of T(H)17 cells. *Nature* 453: 1051–1057, 2008. doi:10.1038/nature07036.
5. **Beurel E, Harrington LE, Jope RS.** Inflammatory T helper 17 cells promote depression-like behavior in mice. *Biol Psychiatry* 73: 622–630, 2013. doi:10.1016/j.biopsych.2012.09.021.
6. **Bierer R, Nitta CH, Friedman J, Codianni S, de Frutos S, Dominguez-Bautista JA, Howard TA, Resta TC, Gonzalez Bosc LV.** NFATc3 is required for chronic hypoxia-induced pulmonary hypertension in adult and neonatal mice. *Am J Physiol Lung Cell Mol Physiol* 301: L872–L880, 2011. doi:10.1152/ajplung.00405.2010.
7. **Billon C, Sitaula S, Burris TP.** Inhibition of RORα/γ suppresses atherosclerosis via inhibition of both cholesterol absorption and inflammation. *Mol Metab* 5: 997–1005, 2016. doi:10.1016/j.molmet.2016.07.001.
8. **Bishop JM.** Role of hypoxia in the pulmonary hypertension of chronic bronchitis and emphysema. *Scand J Respir Dis Suppl* 77: 61–65, 1971.
9. **Burke DL, Frid MG, Kunrath CL, Karoor V, Anwar A, Wagner BD, Strassheim D, Stenmark KR.** Sustained hypoxia promotes the development of a pulmonary artery-specific chronic inflammatory microenvironment. *Am J Physiol Lung Cell Mol Physiol* 297: L238–L250, 2009. doi:10.1152/ajplung.90591.2008.
10. **Chang Y, Al-Alwan L, Risse PA, Roussel L, Rousseau S, Halayko AJ, Martin JG, Hamid Q, Eidelman DH.** TH17 cytokines induce human airway smooth muscle cell migration. *J Allergy Clin Immunol* 127: 1046–1053.e2, 2011. doi:10.1016/j.jaci.2010.12.1117.
11. **Cheng X, Yu X, Ding YJ, Fu QQ, Xie JJ, Tang TT, Yao R, Chen Y, Liao YH.** The Th17/Treg imbalance in patients with acute coronary syndrome. *Clin Immunol* 127: 89–97, 2008. doi:10.1016/j.clim.2008.01.009.
12. **Chu Y, Xiangli X, Xiao W.** Regulatory T cells protect against hypoxia-induced pulmonary arterial hypertension in mice. *Mol Med Rep* 11: 3181–3187, 2015. doi:10.3892/mmr.2014.3106.
13. **Cuttica MJ, Langenickel T, Noguchi A, Machado RF, Gladwin MT, Boehm M.** Perivascular T-cell infiltration leads to sustained pulmonary artery remodeling after endothelial cell damage. *Am J Respir Cell Mol Biol* 45: 62–71, 2011. doi:10.1165/rcmb.2009-0365OC.
14. **Dang EV, Barbi J, Yang HY, Jinasena D, Yu H, Zheng Y, Bordman Z, Fu J, Kim Y, Yen HR, Luo W, Zeller K, Shimoda L, Topalian SL, Semenza GL, Dang CV, Pardoll DM, Pan F.** Control of T(H)17/T(reg) balance by hypoxia-inducible factor 1. *Cell* 146: 772–784, 2011. doi:10.1016/j.cell.2011.07.033.
15. **de Frutos S, Spangler R, Alò D, Bosc LV.** NFATc3 mediates chronic hypoxia-induced pulmonary arterial remodeling with alpha-actin up-regulation. *J Biol Chem* 282: 15081–15089, 2007. doi:10.1074/jbc.M702679200.
16. **DeMarco VG, Habibi J, Whaley-Connell AT, Schneider RI, Heller RL, Bosanquet JP, Hayden MR, Delcour K, Cooper SA, Andresen BT, Sowers JR, Dellsperger KC.** Oxidative stress contributes to pulmonary hypertension in the transgenic (mRen2)27 rat. *Am J Physiol Heart Circ Physiol* 294: H2659–H2668, 2008. doi:10.1152/ajpheart.00953.2007.
17. **Dong Z, Yang Y, Zhang T, Li Y, Kang Q, Lei W, Cao Y, Niu X, Wang D, Tai W.** siRNA-Act1 inhibits the function of IL-17 on lung fibroblasts via the NF-κB pathway. *Respiration* 86: 332–340, 2013. doi:10.1159/000348403.
18. **Eid RE, Rao DA, Zhou J, Lo SF, Ranjbaran H, Gallo A, Sokol SI, Pfau S, Pober JS, Tellides G.** Interleukin-17 and interferon-gamma are produced concomitantly by human coronary artery-infiltrating T cells and act synergistically on vascular smooth muscle cells. *Circulation* 119: 1424–1432, 2009. doi:10.1161/CIRCULATIONAHA.108.827618.
19. **Facco M, Zilli C, Siviero M, Ermolao A, Travain G, Baesso I, Bonamico S, Cabrelle A, Zaccaria M, Agostini C.** Modulation of immune response by the acute and chronic exposure to high altitude. *Med Sci Sports Exerc* 37: 768–774, 2005. doi:10.1249/01.MSS.0000162688.54089.CE.
20. **Fröhlich S, Boylan J, McLoughlin P.** Hypoxia-induced inflammation in the lung: a potential therapeutic target in acute lung injury? *Am J Respir Cell Mol Biol* 48: 271–279, 2013. doi:10.1165/rcmb.2012-0137TR.
21. **Gadgil A, Duncan SR.** Role of T-lymphocytes and pro-inflammatory mediators in the pathogenesis of chronic obstructive pulmonary disease. *Int J Chron Obstruct Pulmon Dis* 3: 531–541, 2008. doi:10.2147/COPD.S1759.
22. **Gavett SH, Chen X, Finkelman F, Wills-Karp M.** Depletion of murine CD4+ T lymphocytes prevents antigen-induced airway hyperreactivity and pulmonary eosinophilia. *Am J Respir Cell Mol Biol* 10: 587–593, 1994. doi:10.1165/ajrcmb.10.6.8003337.
23. **Hashimoto-Kataoka T, Hosen N, Sonobe T, Arita Y, Yasui T, Masaki T, Minami M, Inagaki T, Miyagawa S, Sawa Y, Murakami M, Kumanogoh A, Yamauchi-Takihara K, Okumura M, Kishimoto T, Komuro I, Shirai M, Sakata Y, Nakaoka Y.** Interleukin-6/interleukin-21 signaling axis is critical in the pathogenesis of pulmonary arterial hypertension. *Proc Natl Acad Sci USA* 112: E2677–E2686, 2015. doi:10.1073/pnas.1424774112.
24. **Hassoun PM, Mouthon L, Barberà JA, Eddahibi S, Flores SC, Grimminger F, Jones PL, Maitland ML, Michelakis ED, Morrell NW, Newman JH, Rabinovitch M, Schermuly R, Stenmark KR, Voelkel NF, Yuan JXJ, Humbert M.** Inflammation, growth factors, and pulmonary vascular remodeling. *J Am Coll Cardiol* 54, *Suppl*: S10–S19, 2009. doi:10.1016/j.jacc.2009.04.006.
25. **Hautefort A, Girerd B, Montani D, Cohen-Kaminsky S, Price L, Lambrecht BN, Humbert M, Perros F.** T-helper 17 cell polarization in pulmonary arterial hypertension. *Chest* 147: 1610–1620, 2015. doi:10.1378/chest.14-1678.
26. **Hong JY, Chung Y, Steenrod J, Chen Q, Lei J, Comstock AT, Goldsmith AM, Bentley JK, Sajjan US, Hershenson MB.** Macrophage activation state determines the response to rhinovirus infection in a mouse model of allergic asthma. *Respir Res* 15: 63, 2014. doi:10.1186/1465-9921-15-63.
27. **Jernigan NL, Paffett ML, Walker BR, Resta TC.** ASIC1 contributes to pulmonary vascular smooth muscle store-operated Ca^{2+} entry. *Am J Physiol Lung Cell Mol Physiol* 297: L271–L285, 2009. doi:10.1152/ajplung.00020.2009.
28. **Kimura A, Kishimoto T.** IL-6: regulator of Treg/Th17 balance. *Eur J Immunol* 40: 1830–1835, 2010. doi:10.1002/eji.201040391.
29. **Kimura A, Naka T, Kishimoto T.** IL-6-dependent and -independent pathways in the development of interleukin 17-producing T helper cells. *Proc Natl Acad Sci USA* 104: 12099–12104, 2007. doi:10.1073/pnas.0705268104.
30. **Lee Y, Awasthi A, Yosef N, Quintana FJ, Xiao S, Peters A, Wu C, Kleinewietfeld M, Kunder S, Hafler DA, Sobel RA, Regev A, Kuchroo VK.** Induction and molecular signature of pathogenic TH17 cells. *Nat Immunol* 13: 991–999, 2012. doi:10.1038/ni.2416.
31. **Lindén A.** Interleukin-17 and airway remodelling. *Pulm Pharmacol Ther* 19: 47–50, 2006. doi:10.1016/j.pupt.2005.02.004.
32. **Madhur MS, Lob HE, McCann LA, Iwakura Y, Blinder Y, Guzik TJ, Harrison DG.** Interleukin 17 promotes angiotensin II-induced hypertension and vascular dysfunction. *Hypertension* 55: 500–507, 2010. doi:10.1161/HYPERTENSIONAHA.109.145094.
33. **Madjdpour C, Jewell UR, Kneller S, Ziegler U, Schwendener R, Booy C, Kläusli L, Pasch T, Schimmer RC, Beck-Schimmer B.** Decreased alveolar oxygen induces lung inflammation. *Am J Physiol Lung Cell Mol Physiol* 284: L360–L367, 2003. doi:10.1152/ajplung.00158.2002.
34. **Martin-Orozco N, Muranski P, Chung Y, Yang XO, Yamazaki T, Lu S, Hwu P, Restifo NP, Overwijk WW, Dong C.** T helper 17 cells promote cytotoxic T cell activation in tumor immunity. *Immunity* 31: 787–798, 2009. doi:10.1016/j.immuni.2009.09.014.
35. **Mombaerts P, Iacomini J, Johnson RS, Herrup K, Tonegawa S, Papaioannou VE.** RAG-1-deficient mice have no mature B and T lymphocytes. *Cell* 68: 869–877, 1992. doi:10.1016/0092-8674(92)90030-G.
36. **Naeije R, Barberà JA.** Pulmonary hypertension associated with COPD. *Crit Care* 5: 286–289, 2001. doi:10.1186/cc1049.
37. **Nitta CH, Osmond DA, Herbert LM, Beasley BF, Resta TC, Walker BR, Jernigan NL.** Role of ASIC1 in the development of chronic hypoxia-induced pulmonary hypertension. *Am J Physiol Heart Circ Physiol* 306: H41–H52, 2014. doi:10.1152/ajpheart.00269.2013.
38. **Norris CA, He M, Kang LI, Ding MQ, Radder JE, Haynes MM, Yang Y, Paranjpe S, Bowen WC, Orr A, Michalopoulos GK, Stolz DB, Mars**

WM. Synthesis of IL-6 by hepatocytes is a normal response to common hepatic stimuli. *PLoS One* 9: e96053, 2014. doi:10.1371/journal.pone.0096053.

39. **Poduri A, Rateri DL, Howatt DA, Balakrishnan A, Moorleghen JJ, Cassis LA, Daugherty A.** Fibroblast Angiotensin II Type 1a Receptors Contribute to Angiotensin II-Induced Medial Hyperplasia in the Ascending Aorta. *Arterioscler Thromb Vasc Biol* 35: 1995–2002, 2015. doi:10.1161/ATVBAHA.115.305995.
40. **Pugliese SC, Poth JM, Fini MA, Olschewski A, El Kasmi KC, Stenmark KR.** The role of inflammation in hypoxic pulmonary hypertension: from cellular mechanisms to clinical phenotypes. *Am J Physiol Lung Cell Mol Physiol* 308: L229–L252, 2015. doi:10.1152/ajplung.00238.2014.
41. **Ramiro-Diaz JM, Nitta CH, Maston LD, Codianni S, Giermakowska W, Resta TC, Gonzalez Bosc LV.** NFAT is required for spontaneous pulmonary hypertension in superoxide dismutase 1 knockout mice. *Am J Physiol Lung Cell Mol Physiol* 304: L613–L625, 2013. doi:10.1152/ajplung.00408.2012.
42. **Rich S, Rabinovitch M.** Diagnosis and treatment of secondary (non-category 1) pulmonary hypertension. *Circulation* 118: 2190–2199, 2008. doi:10.1161/CIRCULATIONAHA.107.723007.
43. **Sada Y, Dohi Y, Uga S, Higashi A, Kinoshita H, Kihara Y.** Non-suppressive regulatory T cell subset expansion in pulmonary arterial hypertension. *Heart Vessels* 31: 1319–1326, 2016. doi:10.1007/s00380-015-0727-4.
44. **Saetta M, Turato G, Maestrelli P, Mapp CE, Fabbri LM.** Cellular and structural bases of chronic obstructive pulmonary disease. *Am J Respir Crit Care Med* 163: 1304–1309, 2001. doi:10.1164/ajrccm.163.6.2009116.
45. **Savale L, Tu L, Rideau D, Izziki M, Maitre B, Adnot S, Eddahibi S.** Impact of interleukin-6 on hypoxia-induced pulmonary hypertension and lung inflammation in mice. *Respir Res* 10: 6, 2009. doi:10.1186/1465-9921-10-6.
46. **Schmittgen TD, Livak KJ.** Analyzing real-time PCR data by the comparative C(T) method. *Nat Protoc* 3: 1101–1108, 2008. doi:10.1038/nprot.2008.73.
47. **Simonneau G, Gatzoulis MA, Adatia I, Celermajer D, Denton C, Ghofrani A, Gomez Sanchez MA, Krishna Kumar R, Landzberg M, Machado RF, Olschewski H, Robbins IM, Souza R.** Updated clinical classification of pulmonary hypertension. *J Am Coll Cardiol* 62, *Suppl*: D34–D41, 2013. doi:10.1016/j.jacc.2013.10.029.
48. **Solt LA, Kumar N, He Y, Kamenecka TM, Griffin PR, Burris TP.** Identification of a selective RORγ ligand that suppresses T(H)17 cells and stimulates T regulatory cells. *ACS Chem Biol* 7: 1515–1519, 2012. doi:10.1021/cb3002649.
49. **Solt LA, Kumar N, Nuhant P, Wang Y, Lauer JL, Liu J, Istrate MA, Kamenecka TM, Roush WR, Vidović D, Schürer SC, Xu J, Wagoner G, Drew PD, Griffin PR, Burris TP.** Suppression of TH17 differentiation and autoimmunity by a synthetic ROR ligand. *Nature* 472: 491–494, 2011. doi:10.1038/nature10075.
50. **Stenmark KR, Davie NJ, Reeves JT, Frid MG.** Hypoxia, leukocytes, and the pulmonary circulation. *J Appl Physiol (1985)* 98: 715–721, 2005. doi:10.1152/japplphysiol.00840.2004.
51. **Steudel W, Ichinose F, Huang PL, Hurford WE, Jones RC, Bevan JA, Fishman MC, Zapol WM.** Pulmonary vasoconstriction and hypertension in mice with targeted disruption of the endothelial nitric oxide synthase (NOS 3) gene. *Circ Res* 81: 34–41, 1997. doi:10.1161/01.RES.81.1.34.
52. **Tada Y, Majka S, Carr M, Harral J, Crona D, Kuriyama T, West J.** Molecular effects of loss of BMPR2 signaling in smooth muscle in a transgenic mouse model of PAH. *Am J Physiol Lung Cell Mol Physiol* 292: L1556–L1563, 2007. doi:10.1152/ajplung.00305.2006.
53. **Tamosiuniene R, Tian W, Dhillon G, Wang L, Sung YK, Gera L, Patterson AJ, Agrawal R, Rabinovitch M, Ambler K, Long CS, Voelkel NF, Nicolls MR.** Regulatory T cells limit vascular endothelial injury and prevent pulmonary hypertension. *Circ Res* 109: 867–879, 2011. doi:10.1161/CIRCRESAHA.110.236927.
54. **Tan Z, Qian X, Jiang R, Liu Q, Wang Y, Chen C, Wang X, Ryffel B, Sun B.** IL-17A plays a critical role in the pathogenesis of liver fibrosis through hepatic stellate cell activation. *J Immunol* 191: 1835–1844, 2013. doi:10.4049/jimmunol.1203013.
55. **Tesmer LA, Lundy SK, Sarkar S, Fox DA.** Th17 cells in human disease. *Immunol Rev* 223: 87–113, 2008. doi:10.1111/j.1600-065X.2008.00628.x.
56. **Vargas-Rojas MI, Ramírez-Venegas A, Limón-Camacho L, Ochoa L, Hernández-Zenteno R, Sansores RH.** Increase of Th17 cells in peripheral blood of patients with chronic obstructive pulmonary disease. *Respir Med* 105: 1648–1654, 2011. doi:10.1016/j.rmed.2011.05.017.
57. **Veldhoen M, Hirota K, Christensen J, O'Garra A, Stockinger B.** Natural agonists for aryl hydrocarbon receptor in culture medium are essential for optimal differentiation of Th17 T cells. *J Exp Med* 206: 43–49, 2009. doi:10.1084/jem.20081438.
58. **Yang XO, Pappu BP, Nurieva R, Akimzhanov A, Kang HS, Chung Y, Ma L, Shah B, Panopoulos AD, Schluns KS, Watowich SS, Tian Q, Jetten AM, Dong C.** T helper 17 lineage differentiation is programmed by orphan nuclear receptors RORα and RORγ. *Immunity* 28: 29–39, 2008. doi:10.1016/j.immuni.2007.11.016.
59. **Yoon JH, Sudo K, Kuroda M, Kato M, Lee IK, Han JS, Nakae S, Imamura T, Kim J, Ju JH, Kim DK, Matsuzaki K, Weinstein M, Matsumoto I, Sumida T, Mamura M.** Phosphorylation status determines the opposing functions of Smad2/Smad3 as STAT3 cofactors in TH17 differentiation. *Nat Commun* 6: 7600, 2015. doi:10.1038/ncomms8600.
60. **Zhu X, Gadgil AS, Givelber R, George MP, Stoner MW, Sciurba FC, Duncan SR.** Peripheral T cell functions correlate with the severity of chronic obstructive pulmonary disease. *J Immunol* 182: 3270–3277, 2009. doi:10.4049/jimmunol.0802622.